Author Manuscript

Author Manuscript

Author Manuscript

Author Manuscript

HHS Public Access

Author manuscript

Cell Rep. Author manuscript; available in PMC 2024 April 12.

Published in final edited form as:

Cell Rep. 2024 March 26; 43(3): 113904. doi:10.1016/j.celrep.2024.113904.

Disease-causing Slack potassium channel mutations produce opposite effects on excitability of excitatory and inhibitory neurons

Jing Wu[1], **Imran H. Quraishi**[2], **Yalan Zhang**[1], **Mark Bromwich**[1], **Leonard K. Kaczmarek**[1,3,4,*]

[1]Department of Pharmacology, Yale School of Medicine, New Haven, CT 06520, USA

[2]Department of Neurology, Yale Comprehensive Epilepsy Center, Yale School of Medicine, New Haven, CT 06520, USA

[3]Department of Cellular and Molecular Physiology, Yale School of Medicine, New Haven, CT 06520, USA

[4]Lead contact

SUMMARY

The *KCNT1* gene encodes the sodium-activated potassium channel Slack (KCNT1, $K_{Na}1.1$), a regulator of neuronal excitability. Gain-of-function mutations in humans cause cortical network hyperexcitability, seizures, and severe intellectual disability. Using a mouse model expressing the *Slack-R455H* mutation, we find that Na^+-dependent K^+ (K_{Na}) and voltage-dependent sodium (Na_V) currents are increased in both excitatory and inhibitory cortical neurons. These increased currents, however, enhance the firing of excitability neurons but suppress that of inhibitory neurons. We further show that the expression of Na_V channel subunits, particularly that of $Na_V1.6$, is upregulated and that the length of the axon initial segment and of axonal Na_V immunostaining is increased in both neuron types. Our study on the coordinate regulation of K_{Na} currents and the expression of Na_V channels may provide an avenue for understanding and treating epilepsies and other neurological disorders.

In brief

Wu et al. show that increased potassium and sodium currents lead to hyperexcitability in excitatory neurons while suppressing excitability in inhibitory interneurons in a childhood epilepsy mouse model caused by a Slack gain-of-function mutation. Unlike in heterologous systems, this mutation significantly alters sodium channel expression, elongating axonal initial segments.

This is an open access article under the CC BY-NC license (http://creativecommons.org/licenses/by-nc/4.0/).

[*]**Correspondence**: leonard.kaczmarek@yale.edu.

AUTHOR CONTRIBUTIONS

Conceptualization, J.W. and L.K.K. Methodology, J.W., I.H.Q., Y.Z., and L.K.K. Formal analysis, J.W. and L.K.K. Investigation, J.W., I.H.Q., and M.B. Writing – original draft, J.W. and L.K.K. Writing – review & editing, J.W. and L.K.K. Supervision, L.K.K. Funding acquisition, L.K.K.

SUPPLEMENTAL INFORMATION

Supplemental information can be found online at https://doi.org/10.1016/j.celrep.2024.113904.

DECLARATION OF INTERESTS

The authors declare no competing interests.

Author Manuscript
Author Manuscript
Author Manuscript
Author Manuscript

Graphical Abstract

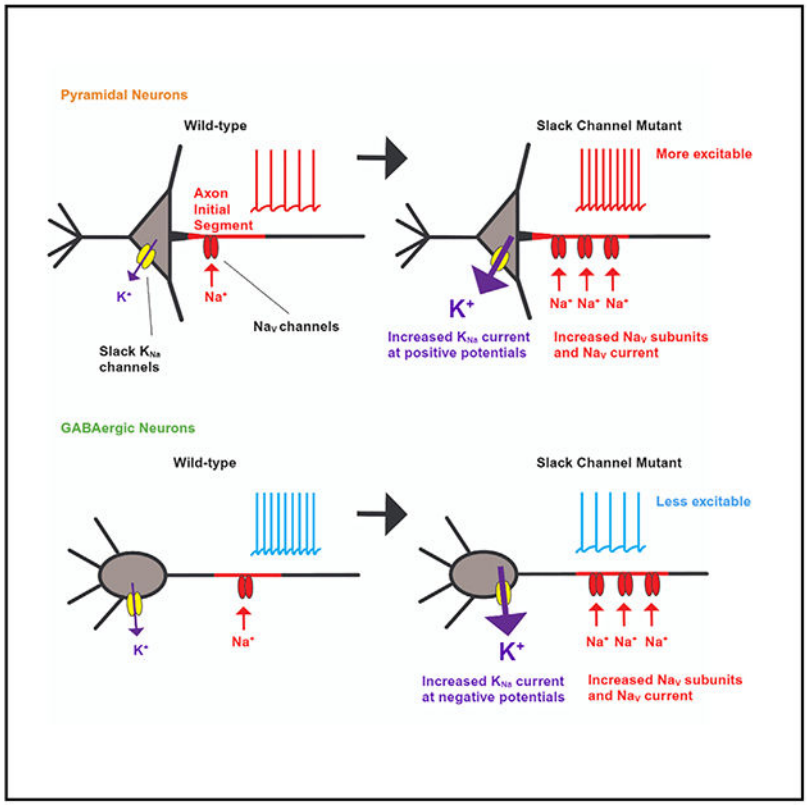

INTRODUCTION

Epilepsy and intellectual disability (ID) are common neurological disorders, with an approximate prevalence of 0.3–2%.[1] Autosomal dominant pathogenic variants in the gene encoding the Na^+-activated K^+ (K_{Na}) channel Slack (KCNT1, $K_{Na}1.1$) have emerged as an important cause of epilepsy and ID with a wide phenotypic spectrum, including epilepsy of infancy with migrating focal seizures (EIMFS) and autosomal dominant nocturnal frontal lobe epilepsy.[2,3] These variants have been shown to increase peak potassium current magnitude and produce gain of function (GOF), leading to network hyperexcitability and seizures.[2–5] The underlying molecular mechanisms have, however, yet to be determined.

Slack channels are highly expressed in the nervous system, including the olfactory bulb, cortex, hippocampus, thalamus, midbrain, cerebellum, and brainstem.[6,7] The Slack channel has two isoforms, Slack-A and Slack-B, which differ only at their N-terminal cytoplasmic domain.[8] Within the cortex, Slack-B, a major splice isoform, is predominantly expressed in the frontal cortex,[7] whereas Slack-A is expressed at higher levels throughout the cortex.[8] Moreover, mRNA for Slack is found in neurons throughout the cortex. Slack channels play crucial roles in regulating the intrinsic excitability of neurons in multiple ways. In physiological conditions, the K_{Na} currents mediated by Slack channels can reduce neuronal excitability by activating in response to small depolarizations at the resting membrane

Author Manuscript Author Manuscript Author Manuscript Author Manuscript

potential[9,10] or increase excitability by activating rapidly during an action potential (AP), which speeds up AP repolarization, thereby limiting Na channel inactivation and causing a higher AP firing frequency.[5,11–14] The effect of a *Slack* variant on the patterns of excitability of a specific cell therefore depends on which of these two effects take place.

Cortical networks are composed of two primary types of neurons: glutamatergic excitatory pyramidal neurons and GABAergic inhibitory interneurons, which work together to regulate many processes, including tuning the overall network excitability of the brain.[15,16] Epilepsy has been causally linked to altered excitation/inhibition neuronal balance. Enhanced excitation in excitatory neurons and/or inhibition in inhibitory interneurons results in hyperactivity of the epileptic circuitry.[17,18] Two recent studies have shown that excitability and AP generation of inhibitory interneurons, but not excitatory neurons, were impaired by *Slack* GOF variants, leading to the loss of inhibitory regulation and seizure susceptibility,[13,14] suggesting that *Slack* GOF variants may have different effects on the excitability of the two specific neuron types. In contrast to the situation in humans, where a mutation in a single copy of the *Slack* (*Kcnt1*) gene results in serious disease, the mouse models used in these studies were homozygous for the channel mutations.

We have generated and characterized a mouse model of EIMFS that bears the *Slack-R455H* mutation (*R474H* in human numbering).[19] Previous work has demonstrated that this variant produces greatly increased K_{Na} current, together with a shift in voltage dependence to negative potentials when expressed in heterologous cells.[3,4] Mice bearing a homozygous *Slack-R455H* mutation are stillborn, but the heterozygotes survive. These heterozygote $Slack^{+/R455H}$ animals, however, have persistent interictal spikes, spontaneous seizures, and an increased susceptibility to pentylenetetrazole-induced seizures,[19] matching the condition for human EIMFS. In the present study, we tested whether the *Slack-R455H* GOF variant leads to network hyperexcitability and produces early-onset seizures by enhancing excitation in excitatory neurons or suppressing excitability in inhibitory interneurons. We determined that the *Slack-R455H* mutation results in increased K_{Na} and Na^+ currents in both cell types, with opposite effects on the excitability of the two neuron types, and that these enhanced currents are coupled to increased expression of Na_V channels and axon initial segment (AIS) length. Our study provides insight into the pathogenesis of epilepsies and associated ID in patients with Slack GOF mutations and may lead to methods and targets for treating neurodevelopmental diseases and other neurological disorders.

RESULTS

Slack channels are expressed in cortical excitatory glutamatergic and inhibitory GABAergic neurons

To understand the mechanisms and consequences of *Slack* GOF mutations in the neuronal excitability of specific cell types, we generated a mouse model of Slack-associated EIMFS with the *Slack-R455H* missense mutation in exon 15 that lies within a regulator of potassium conductance domain of the Slack channel, as described previously[19] (Figure S1A). For some experiments, the $Slack^{+/R455H}$ mouse line was crossed with a GAD67-GFP mouse line that selectively expresses EGFP in the parvalbumin-expressing interneurons for identifying and targeting these GABAergic neurons. Under epifluorescence microscopy, the green

Author Manuscript Author Manuscript Author Manuscript Author Manuscript

fluorescence of interneurons can be readily detected in cultured cortical neurons on days *in vitro* (DIV) 14 and in the cerebral cortex of 2-month-old mice (Figure S1A).

We first carried out immunolocalization to examine the expression of Slack channels in cultured cortical neurons. Co-staining with antibodies against GluR1 and GAD67, biomarkers for glutamatergic and GABAergic neurons, respectively, we observed that Slack channels are highly expressed in both glutamatergic and GABAergic neurons (Figure 1A). Slack channels are expressed at the cell body and dendrites of the neurons, as indicated by its colocalization with microtubule-associated protein 2 (MAP2), a dendritic marker (Figure 1A). Moreover, the morphological features of the glutamatergic and GABAergic neurons in primary culture are different. Consistent with previous studies,[20–22] $GluR1^+$ cultured neurons have a bulbous, triangular cell body with prominent proximal dendrites and an apical dendrite arising from the apex of the cell body, whereas $GAD67^+$ interneurons have a fusiform soma with a bipolar morphology (Figure 1A). We also carried out immunolocalization experiments on the cerebral cortex of intact mouse brains. Using two previously validated anti-Slack cytoplasmic, C-terminal antibodies,[14,23] we identified channel expression in cell bodies in layers II–V of the frontal cortex but not in the somata of cells of layer I (Figures 1B and S1B), and observed colocalization with GluR1 and GAD67 expression within the frontal cortex (Figure 1C). In the intact brain, the expression pattern appears slightly different from that of the cultured cells in that Slack channels have higher expression levels at the soma, with a partial expression extending to the somatodendritic region and the proximal AIS of the cells (Figures 1B and S1B).

To test whether the *Slack-R455H* variant alters the expression of markers for glutamatergic and GABAergic neurons, we measured the protein levels of Slack, GluR1, and GAD67 in the cultured cortical neurons and cerebral cortex from wild-type (WT) and *Slack-R455H* mutant mice by western blotting analysis. Protein lysates of cortical neurons obtained from WT, $Slack^{+/R455H}$, or $Slack^{R455H/R455H}$ littermates (the homozygotes do not survive birth, but cultured neurons from embryos are viable) on DIV 14 showed that there are no significant differences in protein levels of Slack, GluR1, and GAD67 among these cultures (Figure 1D). Similarly, protein levels of Slack, GluR1, and GAD67 in the cerebral cortices obtained from 2-month-old WT and $Slack^{+/R455H}$ mice also show no differences (Figure 1E), suggesting that the *Slack-R455H* mutation does not grossly alter the expression of markers for glutamatergic and GABAergic neurons.

K_{Na} currents and voltage-dependent Na currents (I_{Na} and I_{NaP}) are increased by the *Slack-R455H* mutation in both glutamatergic and GABAergic neurons

Disease-causing mutations in Slack have been shown to cause remarkable increases in K_{Na} currents in heterologous cells, with no change in the levels of Slack protein in the plasma membrane.[3,4] To determine whether K_{Na} currents are increased by the *Slack-R455H* mutation in specific types of neurons, we performed whole-cell voltage recordings of cortical neurons obtained from WT, $Slack^{+/R455H}$, or $Slack^{R455H/R455H}$ embryos (embryonic days [E]16–17) at DIV 13–14. In comparison to other studies using cultures from littermates at postnatal days 0–1 (P0–1),[13] the neurons in the present investigation are indicative of an earlier developmental stage,[26,27] aligning with the conditions for human EIMFS, which

Author Manuscript Author Manuscript Author Manuscript Author Manuscript

manifests at an early developmental age. The recorded cortical neurons were classified as glutamatergic, fast-spiking (FS)-GABAergic, or non-FS (NFS)-GABAergic based on several criteria, including (1) green fluorescent label in GABAergic interneurons (Figure S1A), (2) morphology,[20–22] (3) postimmunolabeling for GluR1 and GAD67 (Figure 1A), and (4) firing patterns.[13,28] To isolate the K_{Na} currents, whole-cell voltage recordings were performed using physiological extracellular medium with 140 mM Na^+ ions and with *N*-methyl-D-glucamine substituted for Na^+. The traces obtained without Na^+ were then subtracted from the traces obtained in the external Na^+ medium.[5]

We observed that K_{Na} currents in both glutamatergic and GABAergic neurons are markedly increased by the *Slack-R455H* mutation (Figures 2A–2C) and that the peak K_{Na} density is increased by as much as 2- to 4-fold in heterozygous neurons and 4- to 6-fold in homozygous neurons over that in WT neurons (Figure 2D). Because sodium entry through voltage-dependent Na channels is a major contributor to K_{Na} currents,[13,29–31] we applied the Na channel blocker tetrodotoxin (TTX) in independent experiments and compared the reduction of K^+ currents in the different genotypes. After subtracting the traces obtained with TTX from those without TTX, we observed that TTX-sensitive K^+ currents in the neurons expressing *Slack-R455H* mutation are larger than in WT neurons (Figures S1C and S1D). The difference current is increased by the *Slack-R455H* mutation by as much as 3-fold in homozygous neurons and 2-fold in heterozygous neurons over that in WT neurons (Figure S1E).

We also observed that the characteristics of the increase in K_{Na} current induced by the *Slack-R455H* mutation are different in glutamatergic and GABAergic neurons. In glutamatergic neurons, significant increases in K_{Na} current only occur in response to depolarization to positive membrane potentials, between +20 and +50 mV in heterozygous neurons and between 0 and +50 mV in homozygous neurons (Figure 2A). In contrast, significant increases in K_{Na} current in FS-GABAergic neurons occur in response to more negative voltage steps, to between −10 and +50 mV in heterozygous neurons and between −30 and +50 mV in homozygous neurons (Figure 2B). In the other class of interneurons, NFS-GABAergic neurons, K_{Na} currents are also increased at more negative potentials, between 0 and +50 mV in heterozygous neurons and between −20 and +50 mV in homozygous neurons (Figure 2C). Overall, the voltage-clamp recording results suggested that although the *Slack-R455H* mutation increases K_{Na} currents in all neuron types, increased K_{Na} currents at subthreshold voltages occur selectively in GABAergic neurons.

A surprising result was that in addition to increased peak K_{Na} current density (Figure 2D), we found that peak transient Na^+ current (I_{Na}) density is increased in all neuron types expressing the *Slack-R455H* mutation, by 2-fold in heterozygous neurons, and by 3-fold in homozygous neurons over that in WT neurons (Figure 2E). Previous studies demonstrated that the activation of K_{Na} channels can also be functionally coupled with Na influx through the persistent Na^+ current (I_{NaP}).[32,33] To further determine whether the *Slack-R455H* mutation also leads to an increase in I_{NaP}, we carried out voltage-clamp recording using slow (30 mV/s) depolarizing voltage ramps ranging from −80 to 10 mV. These measurements were carried out under conditions in which K^+ and Ca^{2+} conductances were blocked pharmacologically. Current-voltage curves for I_{NaP} were obtained from the

Author Manuscript Author Manuscript Author Manuscript Author Manuscript

differences between current amplitude before and after application of TTX (0.5 μM) (Figures 2F and 2I). We observed that the *Slack-R455H* mutation induces a significant increase in I_{NaP} in both glutamatergic neurons and GABAergic neurons. In glutamatergic neurons, significant increases occur between −35 and 0 mV in heterozygous neurons and between −40 and +5 mV in homozygous neurons (Figure 2G), whereas in GABAergic neurons, significant increases occur between −30 and 0 mV in heterozygous neurons and between −35 and +10 mV in homozygous neurons (Figure 2J). In addition, the INaP current density measured at the peak is significantly higher in *Slack-R455H* mutation neurons compared to WT neurons (Figures 2H and 2K). Overall, however, the increases in INaP are smaller than the corresponding increase in peak INa current (for glutamatergic neurons in homozygotes, increases in current densities are 1.763-fold for I_{NaP} vs. 3.074-fold for I_{Na} [n = 10–15 neurons, p = 0.0039, Student's t test]; for GABAergic neurons, increases are 1.795-fold for I_{NaP} density vs. 3.378-fold for peak I_{Na} [n = 10–27 neurons, p = 0.0013, Student's t test]). Collectively, the results indicate that not only K_{Na} currents but also Na^+ currents in cortical neurons are altered by the *Slack-R455H* mutation.

The *Slack-R455H* mutation enhances the excitability of excitatory neurons but suppresses inhibitory interneurons

To investigate further the effects of the *Slack-R455H* mutation GOF on the excitability of specific neuron types, we carried out whole-cell current clamp recordings on cortical neurons from WT, *Slack*$^{+/R455H}$, or *Slack*$^{R455H/R455H}$ embryos at DIV 13–14. The electrophysiological properties of neurons were determined by injecting 200-ms square current pulses incrementing in 20 pA steps, starting at −20 pA. In addition, to compare the maximum number of APs that could be evoked, longer (1.5 s) current pulses in 20 pA steps were injected until the number of APs per stimulus reached a plateau.

We compared the firing properties of glutamatergic neurons from different genotypes. We observed that AP half-width is decreased and afterhyperpolarization (AHP) is increased in the neurons expressing *Slack-R455H* mutation when compared with WT neurons (Figures 3A, 3C, and 3D). However, rheobase, input resistance, and resting membrane potential show no significant differences among all three genotypes (Figures 3E, 3F, and S2A). Other electrophysiological parameters, including AP amplitude, AP depolarization rate, and AP repolarization rate, are increased by the *Slack-R455H* variant in glutamatergic neurons (Figures 3B, S2C, and S2D). Furthermore, the frequency of APs evoked by 1.5-s depolarizing currents is greatly increased in the *Slack-R455H* mutant neurons relative to that of WT neurons (Figures 3G and 3H). Significant increases in AP frequency occur in response to depolarizing currents between 240 and 260 pA in heterozygous neurons and between 160 and 280 pA in homozygous neurons (Figure 3H). In addition, the maximum firing rate that can be evoked in *Slack*$^{R455H/R455H}$ neurons is twice that in WT neurons, whereas *Slack*$^{+/R455H}$ neurons are capable of firing at a rate 1.5-fold over that in WT neurons (Figure 3I).

We next compared the firing properties of GABAergic neurons from the different genotypes. In contrast to glutamatergic neurons, there are no changes in AP half-width or AHP in FS-GABAergic neurons among all three genotypes (Figures 4A, 4C, and 4D). The input

Author Manuscript Author Manuscript Author Manuscript Author Manuscript

resistance is, however, decreased, whereas the rheobase is increased in both the *Slack*$^{+/R455H}$ heterozygous and *Slack*$^{R455H/R455H}$ homozygous neurons when compared with WT neurons (Figures 4E and 4F). Moreover, these neurons have a more hyperpolarized resting membrane potential and AP threshold (Figures S2E and S2F). Again, in contrast to the excitatory neurons, the frequency of APs evoked by 1.5-s depolarizing currents is decreased in the *Slack-R455H* mutant neurons relative to that of WT neurons (Figures 4G–4I). Significant decreases in AP frequency occur in response to depolarizing currents between 180 and 200 pA and between 360 and 400 pA in heterozygous neurons, and between 180 and 260 pA and 340 and 400 pA in homozygous neurons (Figure 4H). The other class of inhibitory neurons, the NFS-GABAergic neurons expressing *Slack-R455H* mutation, also show similar alterations in rheobase, input resistance, resting membrane potential, AP threshold, and firing rate to those of the FS-GABAergic neurons (Figures 4N–4R, S2I, and S2J). In addition, several other parameters, including AP amplitude, AP half-width, and AP depolarization rate, show changes in the opposite direction to those in the glutamatergic neurons (Figures 4K, 4L, and S2K).

Overall, the current-clamp recording results indicate that the *Slack-R455H* mutation enhances the excitability of excitatory neurons but suppress that of inhibitory interneurons.

The *Slack-R455H* mutation upregulates the expression of Na_V channel subunits

To investigate the mechanism underlying the increased Na currents in neurons from mice bearing the *Slack-R455H* mutation, we measured protein levels of $Na_V1.1$, $Na_V1.2$, and $Na_V1.6$, three major Na channel isoforms in the CNS, in cultured cortical neurons and cerebral cortex. Western blotting analysis of cell lysates from DIV 14 cortical neurons showed that protein levels of $Na_V1.1$, $Na_V1.2$, and $Na_V1.6$ are upregulated in the *Slack*$^{+/R455H}$ heterozygous neurons and *Slack*$^{R455H/R455H}$ homozygous neurons when compared with WT neurons (Figure 5A). In the cerebral cortex of 2-month-old *Slack*$^{+/R455H}$ mice, only the $Na_V1.6$ subunit level is significantly upregulated (Figure 5B). These results suggest that the upregulation of Na_V subunits in the *Slack-R455H* mutant neurons contributes, at least in part, to the increased Na^+ and K_{Na} currents.

The *Slack-R455H* mutation alters the length of the AIS in both glutamatergic and GABAergic neurons

The increase in the expression of Na_V subunits and Na^+ currents induced by the *Slack-R455H* mutation may be expected to be reflected in the morphology of the AIS. Before quantifying changes in axonal morphology, we carried out coimmunolocalization experiments to localize Slack channels and Na_V channel isoforms *in vitro* and *in vivo*. The AIS and dendrites were identified using antibodies against ankyrin G (AnkG) and MAP2, respectively. In DIV 14 cultures, $Na_V1.1$ colocalizes with Slack in the AIS as well as the soma and dendrites of both glutamatergic and GABAergic neurons (Figure S3A). Consistent with previous reports,[34–37] $Na_V1.2$ and $Na_V1.6$ subunits are highly enriched at the AIS of glutamatergic and GABAergic neurons, where colocalization with Slack channels is detected (Figures 6A and S3B). In the frontal cortex of 2-month-old mice, $Na_V1.1$ and $Na_V1.2$ localize to the AIS of GABAergic interneurons (Figure S4A) or glutamatergic pyramidal neurons (Figure S4B), respectively, whereas $Na_V1.6$ is in the AIS of both cell

Author Manuscript Author Manuscript Author Manuscript Author Manuscript

types (Figure 6B), consistent with previous reports.[36,37] Using a previously validated anti-Slack cytoplasmic C terminus antibody, we found that Slack staining is highly expressed at the soma of cerebral cortical cells (Figure 6B), although in some cases, the channels are also present at the somatodendritic region and the proximal AIS (Figures 1B, 6B, and S4C).

To quantify the dimensions of the AIS, we first measured the length of AnkG immunostaining as well as the diameter of the AIS in primary cortical neurons obtained from WT and mutant mice. In DIV 14 cultures of frontal cortex (Figures 7A and 7B), in which $Na_V1.2$ and $Na_V1.6$ channels are abundant at the AIS, we observed that the AIS length is significantly increased in both excitatory and inhibitory neurons expressing *Slack-R455H* mutant channels when compared to that of neurons with WT channels (Figure 7D). We found no significant differences, however, in the AIS length or diameter between glutamatergic and GABAergic neurons (Figures 7D and 7E).

We also made similar measurements in layer II/III of the frontal cortices of 2-month-old mice (Figures 7A, 7C, and S4D). As in the cultured cells, we found that the length of the AIS is significantly increased in both pyramidal cells and inhibitory interneurons of mice expressing the heterozygous *Slack-R455H* mutation (Figures 7G and S4E). Although no significant difference in AIS length is observed when comparing pyramidal cells and inhibitory interneurons, the AIS diameter is larger in glutamatergic pyramidal cells than in inhibitory neurons (Figures 7G, 7H, and S4E).

To complement these results, we also examined the expression of MAP2 and AnkG proteins in neuronal cultures and cerebral cortex from WT and *Slack-R455H* mutant mice by western blotting analysis. We found that levels of AnkG protein are increased, whereas MAP2 levels are not altered in protein lysates from *Slack-R455H* mutant cultures (Figure 7J) or cerebral cortex (Figure 7K) when compared to WT cultures or animals, which is consistent with the findings in the immunostaining experiments. Taken together, these results suggest that the increased expression of Na channels in the *Slack-R455H* mutation is accommodated by increases in the length of the AIS in both glutamatergic and GABAergic neurons.

Proximity of the AIS to the soma is different in glutamatergic neurons and GABAergic neurons

Because K_{Na} channels are highly expressed at the soma and proximal regions of both excitatory and inhibitory neurons, one factor that could influence their activation, and potentially be altered by mutations, is their proximity to sites of Na^+ influx, including Na_V channels in the AIS. To evaluate this possibility, we analyzed the relative distance between the soma and the AIS in WT and mutant mice (gap length). In DIV 14 cultures, we observed that the distance between the soma and the AIS is significantly longer in GABAergic neurons than in glutamatergic neurons, but that this is not altered significantly by the *Slack-R455H* mutation in either cell type (Figure 7F). Similar findings were also observed in the cerebral cortices of 2-month-old mice, in which the distance of the AIS from the soma (defined as the distance between the soma and beginning of immunostaining against $Na_V1.6$; Figure 7I) is longer in inhibitory neurons than in glutamatergic pyramidal cells but is not affected by the *Slack-R455H* mutation.

Author Manuscript Author Manuscript Author Manuscript Author Manuscript

Slack does not coimmunoprecipitate with Na_V subunits

Rapid local activation of K_{Na} channels could also occur if the channel subunits form a molecular complex with sources of Na^+ influx. To test for a direct interaction of Slack channel with Na_V subunits, we immunoprecipitated Slack channels from mouse cerebral cortex and tested for coimmunoprecipitation of $Na_V1.1$, $Na_V1.2$, and $Na_V1.6$ antibodies by western blotting. Previous studies have shown that the C-terminal domain of Slack channels interacts with a protein network including FMRP (fragile X mental retardation protein), CYFIP1 (cytoplasmic FMRP-interacting protein 1), and Phactr-1 (phosphatase and actin regulator 1).[38–40] Using FMRP and PP1 (protein phosphatase 1, binding protein of Phactr-1) as positive controls, we found that FMRP and PP1 can be readily precipitated by Slack in mouse cortex. Nevertheless, $Na_V1.1$, $Na_V1.2$, and $Na_V1.6$ could not be detected in the Slack immunoprecipitate (Figure 7L), suggesting that Slack channels do not interact directly with $Na_V1.1$, $Na_V1.2$, or $Na_V1.6$ subunits in mouse cortex.

DISCUSSION

We have found that both excitatory and inhibitory neurons of the cerebral cortex of animals expressing a disease-causing mutation in the Slack potassium channel have increased K_{Na} currents and voltage-dependent Na^+ current. Although the GOF Slack mutation does not alter levels of Slack protein either in cultures of cortical neurons or in cerebral cortices of mutant animals, it substantially increases levels of the Na channel subunit $Na_V1.6$ and in the neuronal cultures of $Na_V1.1$ and $Na_V1.2$. The mutation-induced increase in Na channels is associated with longer axonal initial segments and with enhanced expression of AnkG, a key scaffold protein of the AIS. A similar increase in $Na_V1.6$ staining at the AIS, coupled to increased excitability of pyramidal neurons, has been found in a rat model of temporal lobe epilepsy.[41]

Previous studies have demonstrated that disease-causing mutations in the Slack channel, particularly the EIMFS mutation *Slack-R455H*, markedly increases K^+ current in heterologous cells, with no change in the levels of Slack protein in the plasma membrane or RNA stability of the channel.[3,4] Heterologous systems, however, provide very limited information on the impact of these variants on neuronal physiology and network excitability and cannot address the cellular background, variety, and subcellular specializations of neurons.[42] The present study has provided direct evidence that cortical neurons expressing the *Slack-R455H* mutation have increased peak K_{Na} current amplitudes, by as much as 2- to 4-fold in heterozygous neurons and 4- to 6-fold in homozygous neurons over that in WT neurons. The present study also showed that the total level of Slack protein is unaltered in *Slack-R455H* cortical neurons, consistent with a previous study demonstrating that another Slack GOF mutation does not alter the level of Slack in membrane protein fractions isolated from mouse cortex.[13] It has also shown, however, that in neurons, mutation of the channel produces cellular effects beyond a simple increase in potassium current.

Work with heterologous expression systems has revealed some of the diverse factors that contribute to the increased K^+ current in different Slack GOF mutations. These factors include enhanced Na^+ sensitivity, increased channel open probability, and/or interchannel cooperativity.[43,44] In neurons, however, Slack channels can be activated by Na^+ entry

Author Manuscript Author Manuscript Author Manuscript Author Manuscript

through Na_V channels,[33] nonselective cation channels,[45,46] or ionotropic receptors such as AMPA receptors,[47,48] and changes in any of these pathways will also influence K_{Na} currents. Thus, in addition to the increased intrinsic single-channel activity of *Slack-R455H* mutant channels,[43] the increase in Na^+ currents produced by the mutation in neurons provides another mechanism for increased K_{Na} current.

The mechanism by which a GOF in Slack channels increases Na_V channel expression has not yet been established. One hypothesis, however, is that Slack channel activity directly stimulates the translation of mRNAs encoding Na_V subunits. The hypothesis is supported by a recent study showing that reducing the expression of the *Kcnt1* gene by a *Kcnt1* antisense oligonucleotide has a therapeutic effect in mice with a mutation in the $Na_V1.6$ channel.[49] The cytoplasmic C terminus of Slack channels binds FMRP and CYFIP1,[38–40] two established regulators of translation, and the channel coimmunoprecipitates mRNA targets of FMRP,[38] one of which is mRNA for $Na_V1.6$.[50] Slack channels are required for changes in intrinsic excitability that require new protein synthesis[39] and ongoing experiments have found that activation of WT Slack channels stimulates translation of β-actin, another FMRP target.[51] Future studies clearly will be needed to test the hypothesis that Slack activation directly stimulates the synthesis of Na_V subunits.

The change in the intrinsic excitability of both excitatory and inhibitory neurons produced by the GOF Slack mutation clearly results from increases in the level of both K^+ and Na^+ currents.[52] An increase in K^+ current alone can either increase or decrease excitability,[5,53,54] whereas an increase in Na^+ current would normally be expected only to result in increased excitability. Paradoxically, we found that the excitability of excitatory neurons is enhanced by the *Slack-R455H* mutation but that of inhibitory interneurons is suppressed. Because Na^+ currents are increased to a similar extent in both cell types, it is unlikely that this accounts for this difference, although we cannot rule out some contribution from different changes in Na_V subunits. More significantly, however, the voltage dependence of the increased K_{Na} current is different in GABAergic and glutamatergic neurons. It is known that increasing K^+ currents that activate only at positive potentials increases excitability, whereas increasing those that activate at more negative potentials suppresses firing.[53,54] Consistent with this, in GABAergic neurons, significant increases in K_{Na} current are detected at more negative membrane potentials than in glutamatergic neurons, suggesting that the *Slack-R455H* mutation modifies the intrinsic excitability of GABAergic neurons near the resting potential, hyperpolarizing the neurons and reducing excitability.[9,10,13,14] Conversely, in glutamatergic neurons of *Slack-R455H,* the increased K_{Na} current activates selectively at higher membrane potentials such as those reached only during APs, shortening the APs and limiting Na^+ channel inactivation. This effect of increased K_{Na} currents to increase excitability has also been found in human induced pluripotent stem cell-derived neurons expressing another Slack channel mutation.[5]

There are two potential explanations for the opposite effects of increased K_{Na} currents on the excitability of excitatory and inhibitory neurons. The first is that excitatory and inhibitory cortical neurons may express different splice isoforms of KCNT1 channel. The kinetic behaviors of Slack-A and Slack-B isoforms are very different.[8] The Slack-A isoform activates and deactivates very rapidly with voltage. Such rapid activation during an AP is

Author Manuscript Author Manuscript Author Manuscript Author Manuscript

known to increase the rate of repolarization and subsequent rapid AHP. In contrast, the Slack-B isoform activates more slowly and at more negative potentials.[8] An increase in such a slowly activating K^+ current at the resting membrane potential would increase the amount of current needed to evoke APs and reduce excitability. It is possible that excitatory neurons primarily express the rapidly activating Slack-A isoform, whereas inhibitory neurons express the slowly activating B splice isoform channels.

Independent of which splice isoform is expressed, a second factor that could determine whether increased K_{Na} currents promote or suppress hyperexcitability is the proximity of the K_{Na} channels to the source of Na^+ influx. Patch-clamp recordings of clusters of K_{Na} channels at the nodes of myelinated axons suggest that the increase in Na^+ concentration during a single AP is sufficient to activate these channels.[55] Rapid, transient, and very local activation of K_{Na} channels by a large Na^+ transient during an AP would be expected primarily to produce rapid and transient repolarization, enhancing excitability with little effect on resting membrane properties, as we observed for excitatory neurons (Figure 3). In contrast, slower K_{Na} activation by the accumulation of Na^+ from an influx source remote from the K_{Na} channel would be expected to influence resting membrane properties by decreasing input resistance and suppressing repetitive firing, as observed in inhibitory neurons (Figure 4).

Although the light-level immunocytochemistry we carried out on neurons from WT and mutant animals does not have the resolution to differentiate different degrees of colocalization or clustering of Slack channels with Na_V channels at the molecular level, it revealed clear differences in the organization of the AIS in excitatory neurons and inhibitory neurons. The AIS plays a key role in regulating neuronal excitability,[56,57] and previous work has indicated that the organization of the AIS is heterogeneous in cortical neurons.[58] Our studies on the frontal cortex found that the distance between the soma and the AIS is significantly longer in GABAergic interneurons than in pyramidal neurons. Because Slack staining is abundant at the soma, this provides another potential mechanism for differences in the activation of K_{Na} channels in the two types of cells. Although we are not able to detect coimmunoprecipitation of Slack with any of the Na_V subunits, which would support tight colocalization at the molecular level, our work is consistent with previous studies showing that $Na_V1.1$, $Na_V1.2$, and $Na_V1.6$ have distinct cell type specificities and subcellular distributions. Specifically, $Na_V1.2$ and $Na_V1.6$ are highly expressed at the AIS and nodes of Ranvier of excitatory pyramidal neurons, whereas $Na_V1.1$ is more associated with inhibitory interneurons.[34–37] We also found that $Na_V1.2$ and $Na_V1.6$ are highly expressed at the AIS of cultured cortical neurons and that $Na_V1.1$ is expressed at the AIS as well as at the soma and dendrites. Further studies of the chemical and spatial interactions between Slack channels and channels that provide Na^+ influx will be required to resolve some of these issues and provide new therapeutic directions for the treatment of Slack-related epilepsies and intellectual disability.

Limitations of the study

To determine whether KCNT1 GOF mutations have a gene-dose-dependent effect on K_{Na} current and excitability,[52] we examined both heterozygous and homozygous neurons in

Author Manuscript Author Manuscript Author Manuscript Author Manuscript

primary culture in this study. A limitation of our approach is that changes in neuronal connectivity and synaptic transmission were not evaluated. One aspect of seizures produced in humans with mutations in the *KCNT1* gene is that unlike many other epilepsies, seizures initiated in one cortical locus do not generally spread laterally or cross the corpus collosum. Instead, they appear to occur randomly at different cortical loci. To address this aspect, further investigations involving both electrophysiological recordings and imaging in both cortical slices and, more important, in intact brains will be needed to determine whether the changes in intrinsic excitability that we have described result in anatomical and/or synaptic changes that impair long-range connections.

STAR★METHODS

RESOURCE AVAILABILITY

Lead contact—Further information and requests for resources and reagents should be directed to and will be fulfilled by the Lead Contact, Leonard K. Kaczmarek (leonard.kaczmarek@yale.edu).

Materials availability—The Slack$^{+/R455H}$ mouse line is available from the lead contact, Leonard K. Kaczmarek (leonard.kaczmarek@yale.edu), with a completed Materials Transfer Agreement.

Data and code availability

- The published article includes all datasets generated or analyzed during this study.
- This paper does not report original code.
- Any additional information required to reanalyze the data reported in this paper is available from the lead contact upon request.

EXPERIMENTAL MODEL AND STUDY PARTICIPANT DETAILS

Mouse strains—*Slack*$^{+/R455H}$ mice were generated in the C57BL/6J mouse strain using CRISPR/Cas9 via the Yale Genome Editing Center. The generation and basic characterization of this mouse model are available in our previous paper.[19] Heterozygous (WT/R455H, *Slack*$^{+/R455H}$) mice were used as breeding pairs to obtain WT, heterozygous and homozygous (R455H/R455H, *Slack*$^{R455H/R455H}$) embryos for study. Littermates were labeled and genotyped using gene-specific polymerase chain reaction (PCR) on DNA extracted from tail tissues with primers (*Slack* forward primer: 5′-ACAGCTGCGGTGAGTTCAGG-3′; *Slack* reverse primer: 5′-GGGAAGGTTGTCCCAAAGGAGAGC-3′) with standard thermocycler amplification conditions. Following amplification, a restriction cut was performed with the enzyme TaqI-v2 (NEB, R0149S) to distinguish WT (196 and 112 bp products after cut), R455H heterozygous (112, 196, and 308 bp products) and homozygous (308 bp product) alleles. Whenever possible, investigators were blind to the genotype of the mice. GAD67-GFP mice were purchased from Jackson Laboratories (Bar Harbor, MA). For all experiments, male and female littermates were used for each genotype. All experiments were performed in accord

Author Manuscript Author Manuscript Author Manuscript Author Manuscript

with the NIH Guidelines for the Care and Use of Laboratory Animals and approved by Yale University's Institutional Animal Care and Use Committee (IACUC).

Primary cortical neuron culture—Primary cortical neurons were prepared from E16-17 mouse embryos. After isolation of frontal cortex from embryonic brains, neurons were dissociated and seeded (on coverslips inside a 6 well plate: 0.2E6 cells/well) onto plates containing NB plus [Neurobasal medium supplemented with B27 (Invitrogen GIBCO Life Technologies), GlutaMAX (GIBCO), and penicillin/streptomycin (GIBCO)] and 5% FBS (GIBCO). After 2 h incubation, primary cultures were maintained in NB plus without FBS in a 5% CO_2 and 20% O_2 incubator at 37°C. Subsequently, half the medium was replaced every 2 days.

METHOD DETAILS

Immunofluorescence—For immunocytochemistry of primary cortical neurons on DIV 14, coverslips were fixed in 4% paraformaldehyde for 10 min and permeabilized in blocking buffer (0.2% Triton X-100 and 3% normal goat serum in PBS) for 5 min at room temperature. For immunohistochemistry of cerebral cortex from two-month-old mice, mice were deeply anesthetized with ketamine before transcardial perfusion with ice-cold PBS, followed by ice-cold 4% paraformaldehyde (PFA) and 0.1% glutaraldehyde. Brains were immediately removed and sectioned into 100-μm coronal slices on a vibrating microtome (Leica) and post-fixed in 4% PFA overnight at 4°C. Brain slices were then permeabilized and incubated in blocking buffer for 1 h at room temperature. After blocking, sections from DIV 14 cortical neuronal cultures or two-month-old mice were overlaid with primary antibodies overnight at 4°C. Then, the corresponding Alexa Fluor 488-, 546- or 647-conjugated secondary antibodies were applied. Stained sections were mounted with DAPI-containing mounting solution and sealed with glass coverslips.

Quantitation of axon initial segment (AIS) morphology—Confocal imaging was carried out on a Leica SP5 MP. For AIS analysis, three-dimensional z stack images were taken and stitched into tiles to cover the entirety of the neuron of interest. Z-stacks were then loaded in Leica LAS-X. AIS were defined as AnkG-labeled segments in primary cortical neurons and $Na_V1.6$-labeled segments in brain slices, with clearly identifiable start and endpoints. AIS start point was defined as sharply increased AnkG/$Na_V1.6$ signal closest to the soma. AIS endpoint was defined as reduced AnkG/$Na_V1.6$ signal to the point where it could no longer be discerned from the background. AIS that had blunt ends were excluded, as this is likely an artifact of cutting through the AIS during sectioning. The AIS length measurement was performed by carefully tracing the shape of the AIS using segmented line tool in Leica LAS-X. To determine the distance from the soma to the AIS start point, the shortest possible distance between the neuronal soma (identified by DAPI or VGlut1/GAD67 staining) and the most proximal portion of the AIS (identified by AnkG/NaV1.6 staining) was measured using the straight-line tool in Leica LAS-X.[34,59,60] For the assessment of AIS morphology in primary cortical cultures, nine embryos or cultures were used for each genotype. Within each culture, three AISs of glutamatergic or GABAergic neurons were selected for analysis. For the assessment of AIS morphology in brain slices, three male mice, aged two months, were used for each genotype. In Layers II/III of the

Author Manuscript Author Manuscript Author Manuscript Author Manuscript

frontal cortex, three AISs were analyzed per image, and three images were assessed per mouse. This resulted in a total of twenty-seven AISs being analyzed for each genotype and neuron type, both *in vitro* and *in vivo*.

Western blotting and Co-immunoprecipitation (Co-IP)—Protein lysates from DIV 14 cortical neurons and two-month-old mice frontal cortex were prepared using Pierce IP Lysis Buffer (Thermo Scientific) supplemented with complete EDTA-free Protease Inhibitor Cocktail (Millipore Sigma) according to manufacturer's protocol. Protein quantification was performed using Pierce BCA Protein Assay Kit (Thermo Scientific).

For Co-IP experiments, cerebral cortex lysates from WT mice were incubated with 5 mg anti-Slack IgY antibody or IgY control (AvesLabs) overnight at 4°C. 100 μL Anti-IgY PrecipHen beads (AvesLabs) was added to sample and allowed to incubate for 2 h, followed by wash and collection of beads. Beads were transferred to 2x Laemelli-Buffer with 5% beta-mercaptoethanol and incubated at room temperature for 30 min prior to western blotting.[40]

For all immunoblotting experiments, protein samples were electrophoretically separated on an SDS-PAGE gel (4%–15% gradient gel, Bio-Rad) and transferred onto PVDF membranes (0.2 μm pores, Bio-Rad, USA). Blots were blocked in 5% nonfat milk in Tris-buffered saline and Tween 20 (TBST) for 1 h at room temperature and probed with the primary antibody in 5% milk-TSBT overnight at 4°C. After overnight incubation, the blots were washed three times in TBST for 30 min, followed by incubation with corresponding horseradish peroxidase-conjugated secondary antibodies (1:1000; Abcam, UK) at room temperature for 1 h. Protein bands were visualized via enhanced chemiluminescence and quantified with analyzed with ImageJ (NIH) software. Protein levels were normalized by GAPDH protein level followed by normalization to WT level.

Patch clamp recordings—Whole-cell patch-clamp recordings were performed with patch-clamp amplifiers (MultiClamp 700B; Molecular Devices) under the control of pClamp 11 software (Molecular Devices). Data were recorded with a sampling rate at 20 kHz and filtered at 6 kHz. Rs compensation of 70% was used. Primary cortical neurons at DIV 13–14 were recorded at physiological temperature (37°C). For voltage-clamp experiments to measure the K_{Na} currents and TTX-sensitive K^+ currents, recording electrodes were pulled from filamented borosilicate glass pipettes (Sutter Instrument, CA), and had tip resistances between 4 and 6 MΩ when filled with the following internal solution (in mM): 124 K-gluconate, 2 $MgCl_2$, 13.2 NaCl, 1 EGTA, 10 HEPES, 4 Mg-ATP, and 0.3 Na-GTP (pH 7.3, 290–300 mOsm). The extracellular medium contained the following (in mM): either 140 NaCl or 140 N-methyl-D-glucamine (NMDG), 5.4 KCl, 10 HEPES, 10 glucose, 1 $MgCl_2$, and 1 $CaCl_2$ (pH 7.4, 310 mOsm). Neurons were held at −80 mV and given 60 ms voltage pulses in 10 mV steps over a range of −90 to +50 mV. The difference current over the 20 ms at the end of the voltage pulse was considered the steady state K_{Na} current. To isolate the K_{Na} currents, whole-cell voltage recordings were performed using physiological extracellular medium with 140 mM Na^+ ions and without Na^+ (140 mM NMDG). The traces obtained without Na^+ were then subtracted from the traces obtained in the external Na^+ medium.[5] To isolate the TTX-sensitive K^+ currents, current traces from the TTX (0.5

Author Manuscript Author Manuscript Author Manuscript Author Manuscript

μM) solution were subtracted from the current traces obtained from the standard solution to obtain the difference current.[13]

For current-clamp experiments to measure firing properties, neurons were tested by injecting 200 ms square current pulses incrementing in 20 pA steps, starting at −20 pA. Electrophysiological parameters, including AP amplitude, half-width, AHP, RMP, threshold, depolarization rate, repolarization rate, input resistance, and rheobase, was analyzed according to established protocols[5,13] and using the Clampfit 11 inbuilt statistics measurements program. AP threshold was identified as the membrane potential at the inflection point during the rising phase, AP amplitude as the difference between the peak and threshold, and AHP as the difference between the AP threshold and the lowest V_m value within 50 ms. The AP half-width was measured as the width of the AP at half-maximal amplitude. Maximum depolarization and repolarization rates were analyzed using the Clampfit 11 inbuilt statistics measurements program. Input resistance was calculated from the steady state of voltage responses to hyperpolarizing current steps. To compare the maximum number of action potentials (APs), 1.5 s square current pulses in 20 pA steps were injected until the APs per stimulus reached a plateau phase. Rheobase was defined as the minimum current needed to elicit an action potential (AP) during a 1.5 s current injection.

For voltage-clamp experiments to measure the persistent sodium currents (I_{NaP}), the extracellular medium contained the following (in mM): 140 NaCl, 5.4 KCl, 1 $CaCl_2$,1 $MgCl_2$, 10 glucose, and 10 HEPES; 20 tetraethylammonium (TEA)-Cl, 5 CsCl, 0.1 $CdCl_2$; pH was adjusted to 7.3 with CsOH. The intracellular solution contained the following (in mM): 135 CsF, 2 $MgCl_2$, 4 NaCl, and 10 HEPES, at pH 7.3 adjusted with CsOH. For eliciting I_{NaP}, voltage ramps from −80 to +10 mV with a velocity of 30 mV/s were used. In each case, currents were recorded in the absence and in the presence of TTX (0.5 μM). To isolate the I_{NaP}, current traces from the TTX (0.5 μM) solution were subtracted from the current traces obtained from the standard solution to obtain the difference current.[61,62]

QUANTIFICATION AND STATISTICAL ANALYSIS

Normality and variance similarity were measured by GraphPad Prism before we applied any parametric tests. Two-tailed Student’s t test was used for single comparisons between two groups. Other data were analyzed using one-way or two-way ANOVA with Bonferroni correction (parametric) or Kruskal-Wallis with Dunn’s multi comparison correction (non-parametric) depending on the appropriate design. Post hoc comparisons were carried out only when the primary measure showed statistical significance. All data were expressed as mean ± SEM, with statistical significance determined at p values <0.05. In details, *Indicates $p < 0.05$; **$p < 0.01$; ***$p < 0.001$; ****$p < 0.0001$ in all figures.

Supplementary Material

Refer to Web version on PubMed Central for supplementary material.

ACKNOWLEDGMENTS

This research was supported by NIH grant NS102239 to L.K.K.

Author Manuscript Author Manuscript Author Manuscript Author Manuscript

REFERENCES

1. Robertson J, Hatton C, Emerson E, and Baines S (2015). Prevalence of epilepsy among people with intellectual disabilities: A systematic review. Seizure 29, 46–62. 10.1016/j.seizure.2015.03.016. [PubMed: 26076844]
2. Heron SE, Smith KR, Bahlo M, Nobili L, Kahana E, Licchetta L, Oliver KL, Mazarib A, Afawi Z, Korczyn A, et al. (2012). Missensemutations in the sodium-gated potassium channel gene KCNT1 cause severe autosomal dominant nocturnal frontal lobe epilepsy. Nat. Genet 44, 1188–1190. 10.1038/ng.2440. [PubMed: 23086396]
3. Barcia G, Fleming MR, Deligniere A, Gazula VR, Brown MR, Langouet M, Chen H, Kronengold J, Abhyankar A, Cilio R, et al. (2012). De novo gain-of-function KCNT1 channel mutations cause malignant migrating partial seizures of infancy. Nat. Genet 44, 1255–1259. 10.1038/ng.2441. [PubMed: 23086397]
4. Kim GE, and Kaczmarek LK (2014). Emerging role of the KCNT1 Slack channel in intellectual disability. Front. Cell. Neurosci 8, 209. 10.3389/fncel.2014.00209. [PubMed: 25120433]
5. Quraishi IH, Stern S, Mangan KP, Zhang Y, Ali SR, Mercier MR, Marchetto MC, McLachlan MJ, Jones EM, Gage FH, and Kaczmarek LK (2019). An Epilepsy-Associated KCNT1 Mutation Enhances Excitability of Human iPSC-Derived Neurons by Increasing Slack KNa Currents. J. Neurosci 39, 7438–7449. 10.1523/JNEUROSCI.1628-18.2019. [PubMed: 31350261]
6. Rizzi S, Knaus HG, and Schwarzer C (2016). Differential distribution of the sodium-activated potassium channels slick and slack in mouse brain. J. Comp. Neurol 524, 2093–2116. 10.1002/cne.23934. [PubMed: 26587966]
7. Bhattacharjee A, Gan L, and Kaczmarek LK (2002). Localization of the Slack potassium channel in the rat central nervous system. J. Comp. Neurol 454, 241–254. 10.1002/cne.10439. [PubMed: 12442315]
8. Brown MR, Kronengold J, Gazula VR, Spilianakis CG, Flavell RA, von Hehn CAA, Bhattacharjee A, and Kaczmarek LK (2008). Aminotermini isoforms of the Slack K+ channel, regulated by alternative promoters, differentially modulate rhythmic firing and adaptation. J. Physiol 586, 5161–5179. [PubMed: 18787033]
9. Yang B, Desai R, and Kaczmarek LK (2007). Slack and Slick K(Na) channels regulate the accuracy of timing of auditory neurons. J. Neurosci 27, 2617–2627. [PubMed: 17344399]
10. Wallén P, Robertson B, Cangiano L, Löw P, Bhattacharjee A, Kaczmarek LK, and Grillner S (2007). Sodium-dependent potassium channels of a Slack-like subtype contribute to the slow afterhyperpolarization in lamprey spinal neurons. J. Physiol 585, 75–90. [PubMed: 17884929]
11. Du W, Bautista JF, Yang H, Diez-Sampedro A, You SA, Wang L, Kotagal P, Lüders HO, Shi J, Cui J, et al. (2005). Calcium-sensitive potassium channelopathy in human epilepsy and paroxysmal movement disorder. Nat. Genet 37, 733–738. 10.1038/ng1585. [PubMed: 15937479]
12. Yang J, Krishnamoorthy G, Saxena A, Zhang G, Shi J, Yang H, Delaloye K, Sept D, and Cui J (2010). An epilepsy/dyskinesia-associated mutation enhances BK channel activation by potentiating Ca2+ sensing. Neuron 66, 871–883. 10.1016/j.neuron.2010.05.009. [PubMed: 20620873]
13. Shore AN, Colombo S, Tobin WF, Petri S, Cullen ER, Dominguez S, Bostick CD, Beaumont MA, Williams D, Khodagholy D, et al. (2020). Reduced GABAergic Neuron Excitability, Altered Synaptic Connectivity, and Seizures in a KCNT1 Gain-of-Function Mouse Model of Childhood Epilepsy. Cell Rep. 33, 108303. 10.1016/j.celrep.2020.108303. [PubMed: 33113364]
14. Gertler TS, Cherian S, DeKeyser JM, Kearney JA, and George AL Jr. (2022). KNa1.1 gain-of-function preferentially dampens excitability of murine parvalbumin-positive interneurons. Neurobiol. Dis 168, 105713. 10.1016/j.nbd.2022.105713. [PubMed: 35346832]
15. Tremblay R, Lee S, and Rudy B (2016). GABAergic Interneurons in the Neocortex: From Cellular Properties to Circuits. Neuron 91, 260–292. 10.1016/j.neuron.2016.06.033. [PubMed: 27477017]
16. Ferguson BR, and Gao WJ (2018). PV Interneurons: Critical Regulators of E/I Balance for Prefrontal Cortex-Dependent Behavior and Psychiatric Disorders. Front. Neural Circ 12, 37. 10.3389/fncir.2018.00037.

Author Manuscript Author Manuscript Author Manuscript Author Manuscript

17. Shao LR, Habela CW, and Stafstrom CE (2019). Pediatric Epilepsy Mechanisms: Expanding the Paradigm of Excitation/Inhibition Imbalance. Children 6, 23. 10.3390/children6020023. [PubMed: 30764523]

18. Federica F, Giulia V, Giulia Z, Luciano C, and Giorgio M (2020). Advances in the use of GABAergic interneurons for the treatment of epilepsy. Journal of Stem Cell Therapy and Transplantation 3, 9–22.

19. Quraishi IH, Mercier MR, McClure H, Couture RL, Schwartz ML, Lukowski R, Ruth P, and Kaczmarek LK (2020). Impaired motor skill learning and altered seizure susceptibility in mice with loss or gain of function of the Kcnt1 gene encoding Slack (KNa1.1) Na(+)-activated K(+) channels. Sci. Rep 10, 3213. 10.1038/s41598-020-60028-z. [PubMed: 32081855]

20. Rasia-Filho AA, Guerra KTK, Vásquez CE, Dall'Oglio A, Reberger R, Jung CR, andCalcagnotto ME (2021). The Subcortical-Allocortical-Neocortical continuum for the Emergence and Morphological Heterogeneity of Pyramidal Neurons in the Human Brain. Front. Synaptic Neurosci 13, 616607. 10.3389/fnsyn.2021.616607. [PubMed: 33776739]

21. Turko P, Groberman K, Kaiser T, Yanagawa Y, and Vida I (2019). Primary Cell Culture of Purified GABAergic or Glutamatergic Neurons Established through Fluorescence-activated Cell Sorting. J. Vis. Exp 10.3791/58974.

22. Nadadhur AG, Emperador Melero J, Meijer M, Schut D, Jacobs G, Li KW, Hjorth JJJ, Meredith RM, Toonen RF, Van Kesteren RE, et al. (2017). Multi-level characterization of balanced inhibitory-excitatory cortical neuron network derived from human pluripotent stem cells. PLoS One 12, e0178533. 10.1371/journal.pone.0178533. [PubMed: 28586384]

23. Lee JH, Kang M, Park S, Perez-Flores MC, Zhang XD, Wang W, Gratton MA, Chiamvimonvat N, and Yamoah EN (2019). The local translation of K(Na) in dendritic projections of auditory neurons and the roles of K(Na) in the transition from hidden to overt hearing loss. Aging (Albany NY) 11, 11541–11564. 10.18632/aging.102553. [PubMed: 31812952]

24. Manuel M, Georgala PA, Carr CB, Chanas S, Kleinjan DA, Martynoga B, Mason JO, Molinek M, Pinson J, Pratt T, et al. (2007). Controlled overexpression of Pax6 in vivo negatively autoregulates the Pax6 locus, causing cell-autonomous defects of late cortical progenitor proliferation with little effect on cortical arealization. Development 134, 545–555. 10.1242/dev.02764. [PubMed: 17202185]

25. Lemmens MAM, Sierksma ASR, Rutten BPF, Dennissen F, Steinbusch HWM, Lucassen PJ, and Schmitz C (2011). Age-related changes of neuron numbers in the frontal cortex of a transgenic mouse model of Alzheimer's disease. Brain Struct. Funct 216, 227–237. 10.1007/s00429-011-0305-1. [PubMed: 21409417]

26. Sun Z, Williams DJ, Xu B, and Gogos JA (2018). Altered function and maturation of primary cortical neurons from a 22q11.2 deletion mouse model of schizophrenia. Transl. Psychiatry 8, 85. 10.1038/s41398-018-0132-8. [PubMed: 29666363]

27. Goldberg EM, Jeong HY, Kruglikov I, Tremblay R, Lazarenko RM, and Rudy B (2011). Rapid developmental maturation of neocortical FS cell intrinsic excitability. Cerebr. Cortex 21, 666–682. 10.1093/cercor/bhq138.

28. Subkhankulova T, Yano K, Robinson HPC, and Livesey FJ (2010). Grouping and classifying electrophysiologically-defined classes of neocortical neurons by single cell, whole-genome expression profiling. Front. Mol. Neurosci 3, 10. 10.3389/fnmol.2010.00010. [PubMed: 20428506]

29. Reijntjes DOJ, Lee JH, Park S, Schubert NMA, van Tuinen M, Vijayakumar S, Jones TA, Jones SM, Gratton MA, Xia XM, et al. (2019). Sodium-activated potassium channels shape peripheral auditory function and activity of the primary auditory neurons in mice. Sci. Rep 9, 2573. 10.1038/s41598-019-39119-z. [PubMed: 30796290]

30. Cervantes B, Vega R, Limón A, and Soto E (2013). Identity, expression and functional role of the sodium-activated potassium current in vestibular ganglion afferent neurons. Neuroscience 240, 163–175. 10.1016/j.neuroscience.2013.02.052. [PubMed: 23466807]

31. Budelli G, Hage TA, Wei A, Rojas P, Jong YJI, O'Malley K, and Salkoff L (2009). Na+-activated K+ channels express a large delayed outward current in neurons during normal physiology. Nat. Neurosci 12, 745–750. 10.1038/nn.2313. [PubMed: 19412167]

Author Manuscript Author Manuscript Author Manuscript Author Manuscript

32. Skrabak D, Bischof H, Pham T, Ruth P, Ehinger R, Matt L, and Lukowski R (2023). Slack K(+) channels limit kainic acid-induced seizure severity in mice by modulating neuronal excitability and firing. Commun. Biol 6, 1029. 10.1038/s42003-023-05387-9. [PubMed: 37821582]
33. Hage TA, and Salkoff L (2012). Sodium-activated potassium channels are functionally coupled to persistent sodium currents. J. Neurosci 32, 2714–2721. 10.1523/JNEUROSCI.5088-11.2012. [PubMed: 22357855]
34. Liu H, Wang HG, Pitt GS, and Liu ZJ (2022). Direct Observation of Compartment-Specific Localization and Dynamics of Voltage-Gated Sodium Channels. J. Neurosci 42, 5482–5498. 10.1523/JNEUROSCI.0086-22.2022. [PubMed: 35672149]
35. Lorincz A, and Nusser Z (2010). Molecular identity of dendritic voltagegated sodium channels. Science 328, 906–909. 10.1126/science.1187958. [PubMed: 20466935]
36. Hu W, Tian C, Li T, Yang M, Hou H, and Shu Y (2009). Distinct contributions of Na(v)1.6 and Na(v)1.2 in action potential initiation and back-propagation. Nat. Neurosci 12, 996–1002. 10.1038/nn.2359. [PubMed: 19633666]
37. Li T, Tian C, Scalmani P, Frassoni C, Mantegazza M, Wang Y, Yang M, Wu S, and Shu Y (2014). Action potential initiation in neocortical inhibitory interneurons. PLoS Biol. 12, e1001944. 10.1371/journal.pbio.1001944. [PubMed: 25203314]
38. Brown MR, Kronengold J, Gazula VR, Chen Y, Strumbos JG, Sigworth FJ, Navaratnam D, and Kaczmarek LK (2010). Fragile X mental retardation protein controls gating of the sodium-activated potassium channel Slack. Nat. Neurosci 13, 819–821. 10.1038/nn.2563. [PubMed: 20512134]
39. Zhang Y, Brown MR, Hyland C, Chen Y, Kronengold J, Fleming MR, Kohn AB, Moroz LL, and Kaczmarek LK (2012). Regulation of neuronal excitability by interaction of fragile X mental retardation protein with slack potassium channels. J. Neurosci 32, 15318–15327. 10.1523/JNEUROSCI.2162-12.2012. [PubMed: 23115170]
40. Fleming MR, Brown MR, Kronengold J, Zhang Y, Jenkins DP, Barcia G, Nabbout R, Bausch AE, Ruth P, Lukowski R, et al. (2016). Stimulation of Slack K(+) Channels Alters Mass at the Plasma Membrane by Triggering Dissociation of a Phosphatase-Regulatory Complex. Cell Rep. 16, 2281–2288. 10.1016/j.celrep.2016.07.024. [PubMed: 27545877]
41. Hargus NJ, Merrick EC, Nigam A, Kalmar CL, Baheti AR, Bertram EH 3rd, and Patel MK (2011). Temporal lobe epilepsy induces intrinsic alterations in Na channel gating in layer II medial entorhinal cortex neurons. Neurobiol. Dis 41, 361–376. 10.1016/j.nbd.2010.10.004. [PubMed: 20946956]
42. Avanzini G. (2009). Intrinsic Properties of Neocortical Neurons Relevant to Seizure Discharges: The Lesson of Epileptogenic Channelopathies. Encyclopedia of Basic Epilepsy Research 1–3, 644–651.
43. Kim GE, Kronengold J, Barcia G, Quraishi IH, Martin HC, Blair E, Taylor JC, Dulac O, Colleaux L, Nabbout R, and Kaczmarek LK (2014). Human slack potassium channel mutations increase positive cooperativity between individual channels. Cell Rep. 9, 1661–1672. 10.1016/j.celrep.2014.11.015. [PubMed: 25482562]
44. Tang QY, Zhang FF, Xu J, Wang R, Chen J, Logothetis DE, and Zhang Z (2016). Epilepsy-Related Slack Channel Mutants Lead to Channel Over-Activity by Two Different Mechanisms. Cell Rep. 14, 129–139. 10.1016/j.celrep.2015.12.019. [PubMed: 26725113]
45. Lu S, Das P, Fadool DA, and Kaczmarek LK (2010). The slack sodium-activated potassium channel provides a major outward current in olfactory neurons of Kv1.3−/− super-smeller mice. J. Neurophysiol 103, 3311–3319. 10.1152/jn.00607.2009. [PubMed: 20393063]
46. Wu J, El-Hassar L, Datta D, Thomas M, Zhang Y, Jenkins DP, De-Luca NJ, Chatterjee M, Gribkoff VK, Arnsten AF, and Kaczmarek LK (2023). Interaction Between HCN and Slack Channels Regulates mPFC Pyramidal Cell Excitability in Working Memory Circuits. Mol. Neurobiol, 1–16.
47. Nanou E, and El Manira A (2007). A postsynaptic negative feedback mediated by coupling between AMPA receptors and Na+-activated K+ channels in spinal cord neurones. Eur. J. Neurosci 25, 445–450. 10.1111/j.1460-9568.2006.05287.x. [PubMed: 17284185]

Author Manuscript Author Manuscript Author Manuscript Author Manuscript

48. Nanou E, Kyriakatos A, Bhattacharjee A, Kaczmarek LK, Paratcha G, and El Manira A (2008). Na+-mediated coupling between AMPA receptors and KNa channels shapes synaptic transmission. Proc. Natl. Acad. Sci. USA 105, 20941–20946. 10.1073/pnas.0806403106. [PubMed: 19095801]
49. Hill SF, Jafar-Nejad P, Rigo F, and Meisler MH (2023). Reduction of Kcnt1 is therapeutic in mouse models of SCN1A and SCN8A epilepsy. Front. Neurosci 17, 1282201. [PubMed: 37901435]
50. Darnell JC, Van Driesche SJ, Zhang C, Hung KYS, Mele A, Fraser CE, Stone EF, Chen C, Fak JJ, Chi SW, et al. (2011). FMRP stalls ribosomal translocation on mRNAs linked to synaptic function and autism. Cell 146, 247–261. 10.1016/j.cell.2011.06.013. [PubMed: 21784246]
51. Malone TJ, Wu J, Zhang Y, Licznerski P, Chen R, Nahiyan S, Pedram M, Jonas EA, and Kaczmarek LK (2024). Neuronal potassium channel activity triggers initiation of mRNA translation through binding of translation regulators. Preprint at. bioRxiv 10.1101/2024.02.07.579306
52. Shore AN, Alshaima'a MQ, Spitznagel BD, Weaver CD, Emmitte KA, Frankel WN, and Weston MC (2023). Heterozygous expression of a Kcnt1 gain-of-function variant has differential effects on SST-and PV-expressing cortical GABAergic neurons. Preprint at bioRxiv. 10.1101/2023.10.11.561953.
53. Kaczmarek LK, and Zhang Y (2017). Kv3 Channels: Enablers of Rapid Firing, Neurotransmitter Release, and Neuronal Endurance. Physiol. Rev 97, 1431–1468. 10.1152/physrev.00002.2017. [PubMed: 28904001]
54. Kaczmarek LK (2023). Modulation of potassium conductances optimizes fidelity of auditory information. Proc. Natl. Acad. Sci. USA 120, e2216440120. 10.1073/pnas.2216440120. [PubMed: 36930599]
55. Koh DS, Jonas P, and Vogel W (1994). Na(+)-activated K+ channels localized in the nodal region of myelinated axons of Xenopus. J. Physiol 479, 183–197. 10.1113/jphysiol.1994.sp020287. [PubMed: 7799220]
56. Kole MHP, and Stuart GJ (2012). Signal Processing in the Axon Initial Segment. Neuron 73, 235–247. 10.1016/j.neuron.2012.01.007. [PubMed: 22284179]
57. Leterrier C. (2018). The Axon Initial Segment: An Updated Viewpoint. J. Neurosci 38, 2135–2145. 10.1523/Jneurosci.1922-17.2018. [PubMed: 29378864]
58. Höfflin F, Jack A, Riedel C, Mack-Bucher J, Roos J, Corcelli C, Schultz C, Wahle P, and Engelhardt M (2017). Heterogeneity of the Axon Initial Segment in Interneurons and Pyramidal Cells of Rodent Visual Cortex. Front. Cell. Neurosci 11, 332. 10.3389/fncel.2017.00332. [PubMed: 29170630]
59. Yermakov LM, Drouet DE, Griggs RB, Elased KM, and Susuki K (2018). Type 2 Diabetes Leads to Axon Initial Segment Shortening in db/db Mice. Front. Cell. Neurosci 12, 146. 10.3389/fncel.2018.00146. [PubMed: 29937715]
60. Hinman JD, Rasband MN, and Carmichael ST (2013). Remodeling of the axon initial segment after focal cortical and white matter stroke. Stroke 44, 182–189. 10.1161/STROKEAHA.112.668749. [PubMed: 23233385]
61. Hedrich UBS, Liautard C, Kirschenbaum D, Pofahl M, Lavigne J, Liu Y, Theiss S, Slotta J, Escayg A, Dihné M, et al. (2014). Impaired action potential initiation in GABAergic interneurons causes hyperexcitable networks in an epileptic mouse model carrying a human Na(V)1.1 mutation. J. Neurosci 34, 14874–14889. 10.1523/JNEUROSCI.0721-14.2014. [PubMed: 25378155]
62. Caioli S, Candelotti E, Pedersen JZ, Saba L, Antonini A, Incerpi S, and Zona C (2016). Baicalein reverts L-valine-induced persistent sodium current up-modulation in primary cortical neurons. Biochim. Biophys. Acta 1862, 566–575. 10.1016/j.bbadis.2015.12.021. [PubMed: 26721313]

Author Manuscript Author Manuscript Author Manuscript Author Manuscript

Highlights

- Slack GOF increases K^+ currents and voltage-dependent Na^+ (Na_V) currents in cortical neurons
- Slack GOF enhances firing of excitability neurons but suppresses that of inhibitory neurons
- Slack GOF upregulates Na_V channel expression and increases AIS length in cortical neurons
- Proximity of the AIS to the soma is different between excitatory and inhibitory neurons

Author Manuscript Author Manuscript Author Manuscript Author Manuscript

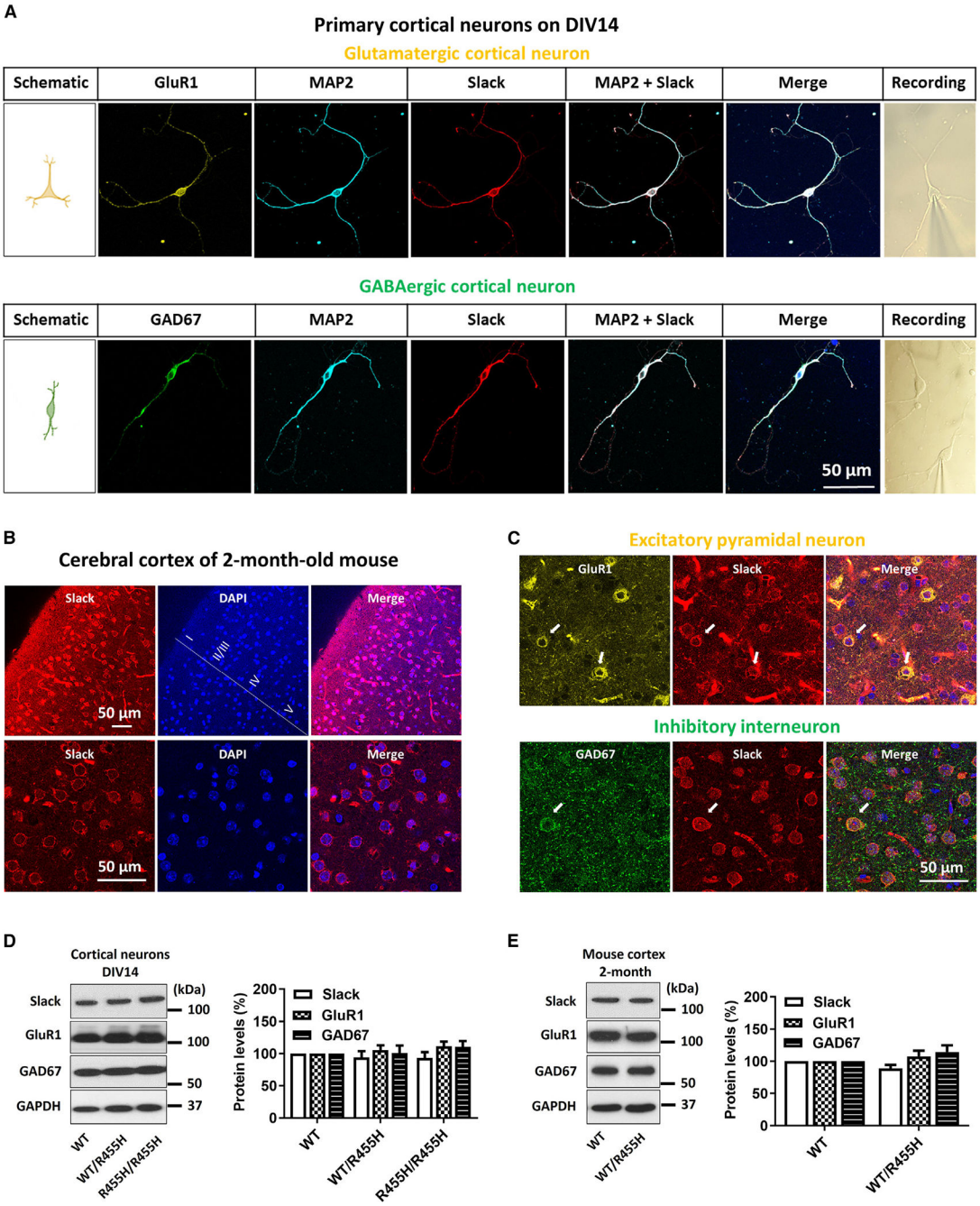

Figure 1. Slack channels are highly expressed in cortical glutamatergic and GABAergic neurons

(A) Immunostaining of Slack channels with GluR1 (biomarker for glutamatergic neurons), GAD67 (biomarker for GABAergic neurons), and MAP2 (biomarker for soma and dendrites) in cultured cortical neurons on DIV 14. Scale bar, 50 μm. The rightmost panels show live light microscopy images (400× magnification) of recorded cortical neurons.

(B) Immunostaining of Slack channels in cerebral cortex of 2-month-old WT mice. The top center panel shows distinct cortical layers identified based on previous studies.[24,25] Scale bar, 50 μm.

Author Manuscript Author Manuscript Author Manuscript Author Manuscript

(C) Immunostaining of Slack channels with GluR1 and GAD67 in cerebral cortex of 2-month-old WT mice. Scale bar, 50 μm.

(D) Representative western blotting and quantitative analysis of protein levels of Slack, GluR1, and GAD67 in cultured cortical neurons on DIV 14. Neuronal cultures were obtained from WT, heterozygous (WT/R455H, $Slack^{+/R455H}$), and homozygous (R455H/R455H, $Slack^{R455H/R455H}$) littermates. Data are shown as mean ± SEM (n = 4 cultures; data are not significant by 1-way ANOVA).

(E) Representative western blotting and quantitative analysis of protein levels of Slack, GluR1, and GAD67 in cerebral cortex of 2-month-old WT and $Slack^{+/R455H}$ mice. Data are shown as mean ± SEM (n = 4 mice; not significant by Student's t test).

See also Figure S1.

Author Manuscript Author Manuscript Author Manuscript Author Manuscript

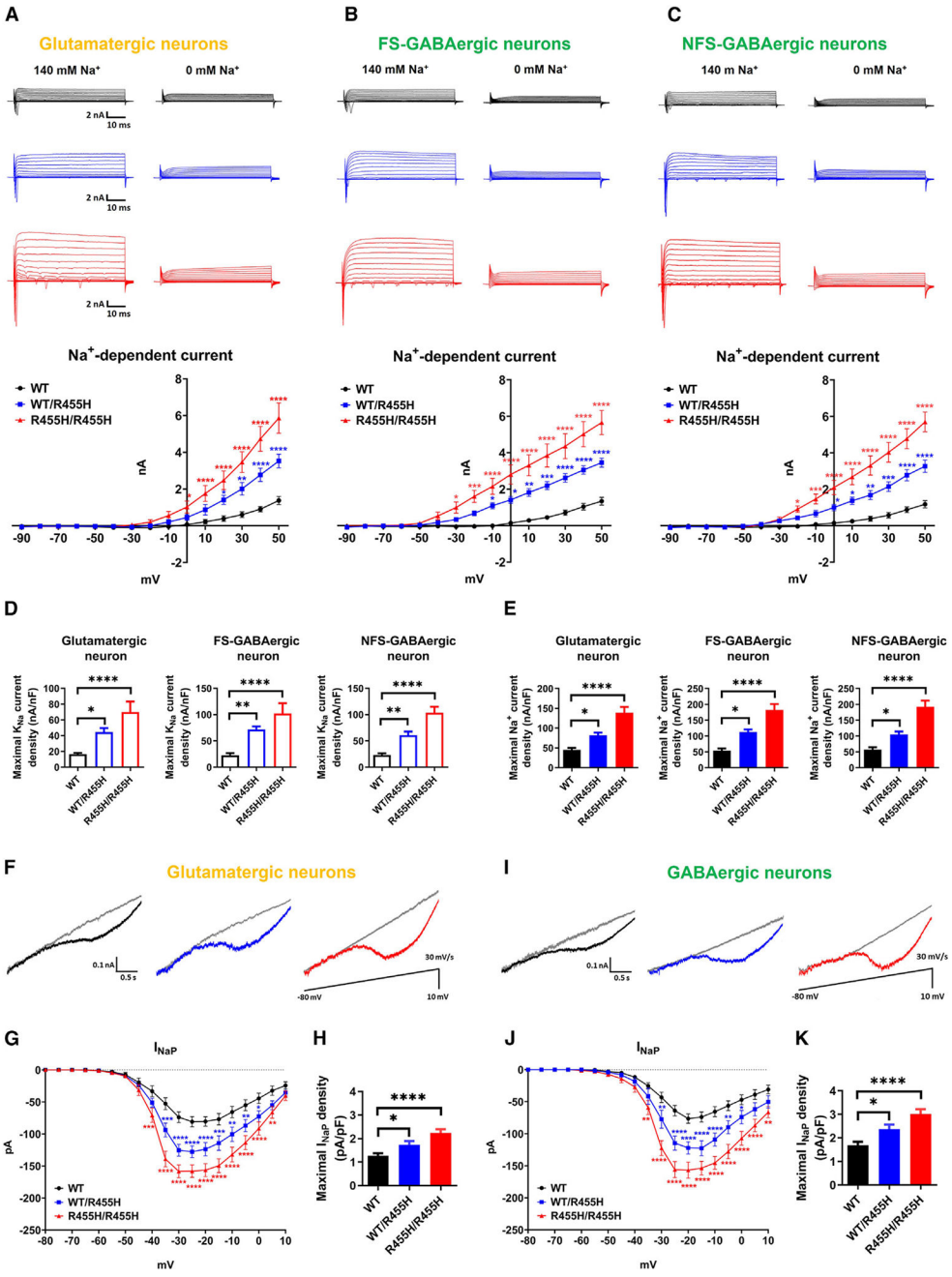

Figure 2. K_{Na} currents, I_{Na} and I_{NaP} are increased in both glutamatergic and GABAergic neurons expressing the *Slack-R455H* mutation

(A–C) Representative current traces from whole-cell voltage-clamp recordings in physiological extracellular medium with 140 mM Na^+ ions (left) and without Na^+ ions (right) in response to voltage steps (−90 to +50 mV) in WT (black), *Slack*$^{+/R455H}$ (blue), and *Slack*$^{R455H/R455H}$ (red) neurons. Summary data (bottom) show the K_{Na} current, which was calculated by subtracting the trace obtained without Na^+ from the trace with Na^+, for each voltage step in glutamatergic neurons (A), FS-GABAergic neurons (B), or NFS-GABAergic neurons (C). Data are shown as mean ± SEM (n = 8–12 neurons, 2-way ANOVA).

Author Manuscript Author Manuscript Author Manuscript Author Manuscript

(D) Maximal K_{Na} current density at +50 mV for each genotype and neuron type. Data are shown as mean ± SEM (n = 8–12 neurons, 1-way ANOVA).
(E) Maximal I_{Na} current density for each genotype and neuron type. Data are shown as mean ± SEM (n = 8–12 neurons, 1-way ANOVA).
(F and I) I_{NaP} traces evoked by a slow voltage ramp protocol (30 mV/s from −80 to +10 mV) in glutamatergic neurons (F) and GABAergic neurons (I) obtained from WT (black), *Slack*$^{+/R455H}$ (blue), and *Slack*$^{R455H/R455H}$ (red) embryos under control conditions and in the presence of 0.5 μM TTX (gray trace).
(G and J) Summary data show the I_{NaP} current, which was calculated by subtracting the trace obtained without TTX from the trace with TTX, at 5-mV intervals for each genotype in glutamatergic neurons (G) and GABAergic neurons (J). Data are shown as mean ± SEM (n = 8–14 neurons, 2-way ANOVA).
(H and K) Maximal I_{NaP} density for each neuron type and genotype. Data are shown as mean ± SEM (n = 8–14 neurons, 1-way ANOVA). *p < 0.05; **p < 0.01; ***p < 0.001; ****p < 0.0001.
See also Figure S1.

Author Manuscript Author Manuscript Author Manuscript Author Manuscript

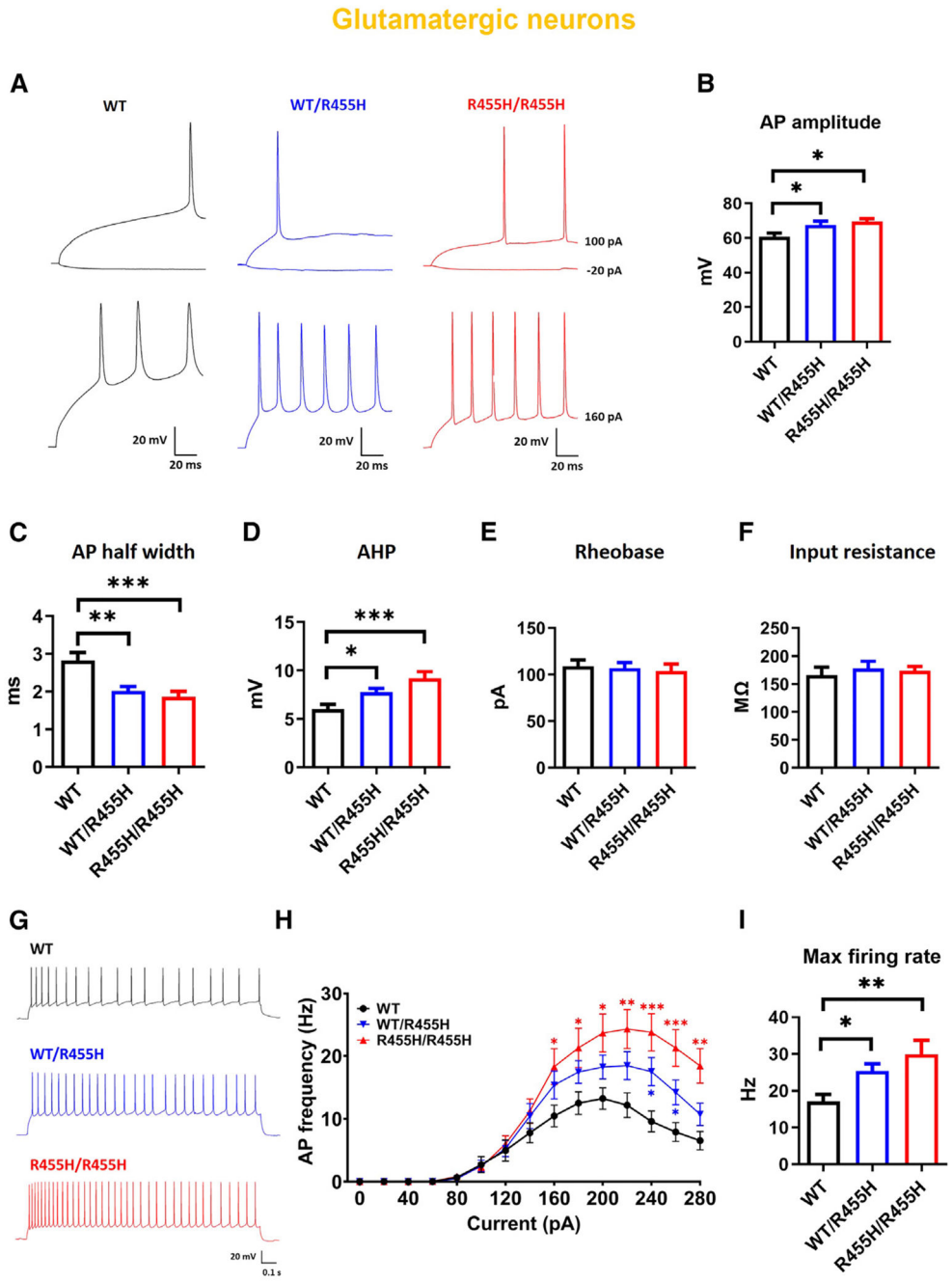

Figure 3. The *Slack-R455H* mutation enhances the excitability of glutamatergic neurons

(A) Representative traces from whole-cell current-clamp recordings from glutamatergic neurons in response to current step injections from WT (black), *Slack*$^{+/R455H}$ (blue), and *Slack*$^{R455H/R455H}$ (red) littermates. To compare the electrophysiological properties, neurons were injected with 200-ms square current pulses in 20-pA step increments, starting at −20 pA. To compare the maximum number of APs, 1.5-s square current pulses in 20-pA steps were injected until the number of APs per stimulus reached a plateau phase.

Author Manuscript Author Manuscript Author Manuscript Author Manuscript

(B–F) AP amplitude (B), AP half-width (C), AHP (D), rheobase (E), and input resistance (F) of recorded neurons from each genotype. Data are shown as mean ± SEM (n = 15–20 neurons, 1-way ANOVA). (G and H) Example traces and summary data showing the frequency of APs per current injection step in WT (black), *Slack*$^{+/R455H}$ (blue), and *Slack*$^{R455H/R455H}$ (red) neurons. Data are shown as mean ± SEM (n = 15–20 neurons, 2-way ANOVA). (I) Maximal firing rate for each genotype. Data are shown as mean ± SEM (n = 15–20 neurons, Kruskal-Wallis test). *p < 0.05; **p < 0.01; ***p < 0.001; ****p < 0.0001. See also Figure S2.

Author Manuscript Author Manuscript Author Manuscript Author Manuscript

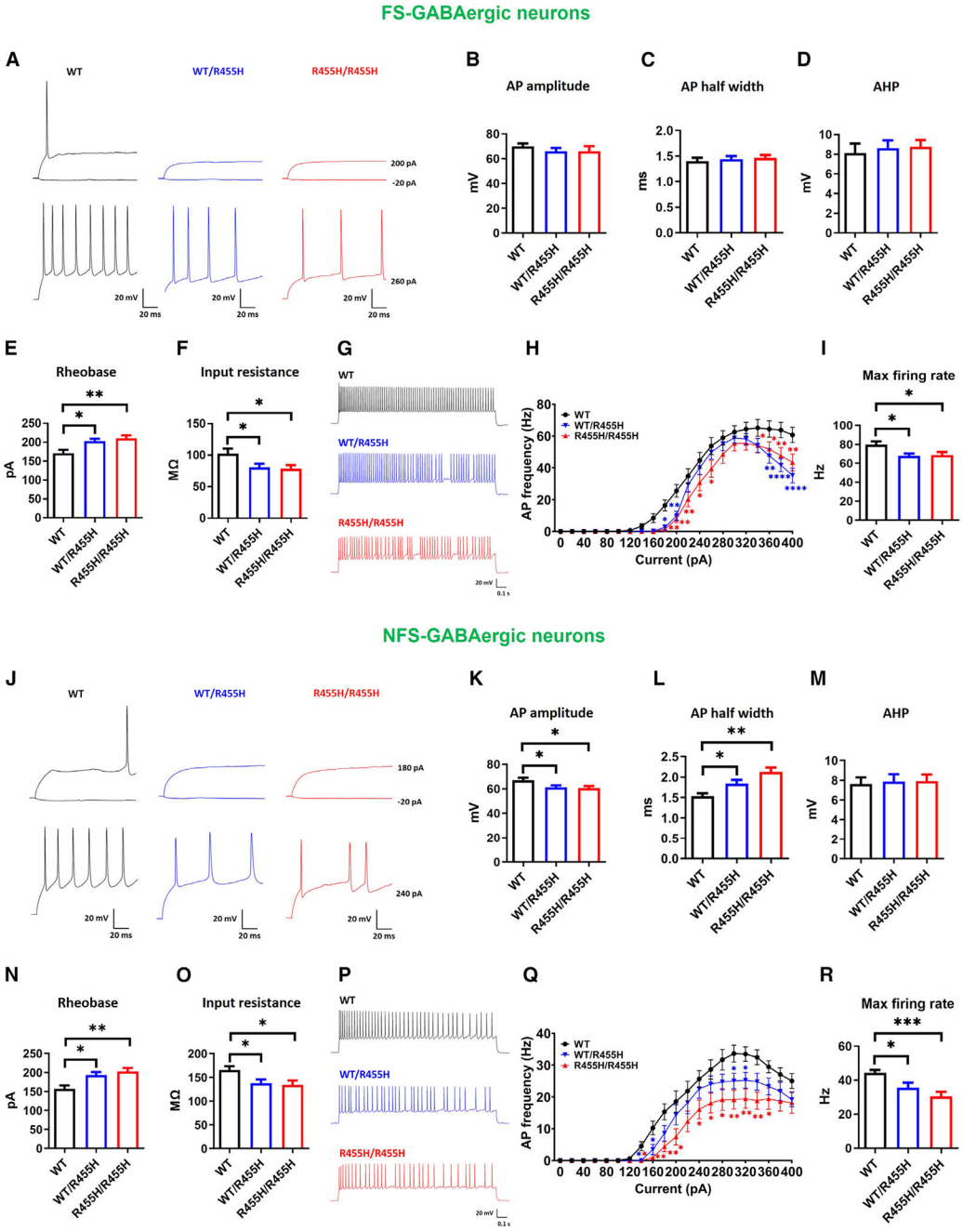

Figure 4. The *Slack-R455H* mutation suppresses the excitability of FS-GABAergic and NFS-GABAergic neurons

(A) Representative traces from whole-cell current-clamp recordings from FS-GABAergic neurons in response to current step injections from WT (black), *Slack*$^{+/R455H}$ (blue), and *Slack*$^{R455H//R455H}$ (red) littermates.

(B–F) AP amplitude (B), AP half-width (C), AHP (D), rheobase (E), and input resistance (F) of recorded neurons from each genotype. Data are shown as mean ± SEM (n = 12–18 neurons, 1-way ANOVA).

Author Manuscript Author Manuscript Author Manuscript Author Manuscript

(G and H) Example traces and summary data showing the frequency of APs per current injection step in WT (black), *Slack*$^{+/R455H}$ (blue), and *Slack*$^{R455H/R455H}$ (red) neurons. Data are shown as mean ± SEM (n = 12–18 neurons, 2-way ANOVA).

(I) Maximal firing rate for each genotype. Data are shown as mean ± SEM (n = 12–18 neurons, Kruskal-Wallis test).

(J) Representative traces from whole-cell current-clamp recordings from NFS-GABAergic neurons in response to current step injections from WT (black), *Slack*$^{+/R455H}$ (blue), and *Slack*$^{R455H/R455H}$ (red) littermates.

(K–O) AP amplitude (K), AP half-width (L), AHP (M), rheobase (N), and input resistance (O) of recorded neurons from each genotype. Data are shown as mean ± SEM (n = 13–17 neurons, 1-way ANOVA).

(P and Q) Example traces and summary data showing the frequency of APs per current injection step in WT (black), *Slack*$^{+/R455H}$ (blue), and *Slack*$^{R455H/R455H}$ (red) neurons. Data are shown as mean ± SEM (n = 13–17 neurons, 2-way ANOVA).

(R) Maximal firing rate for each genotype. Data are shown as mean ± SEM (n = 13–17 neurons, Kruskal-Wallis test). *p < 0.05; **p < 0.01; ***p < 0.001; ****p < 0.0001.

See also Figure S2.

Author Manuscript Author Manuscript Author Manuscript Author Manuscript

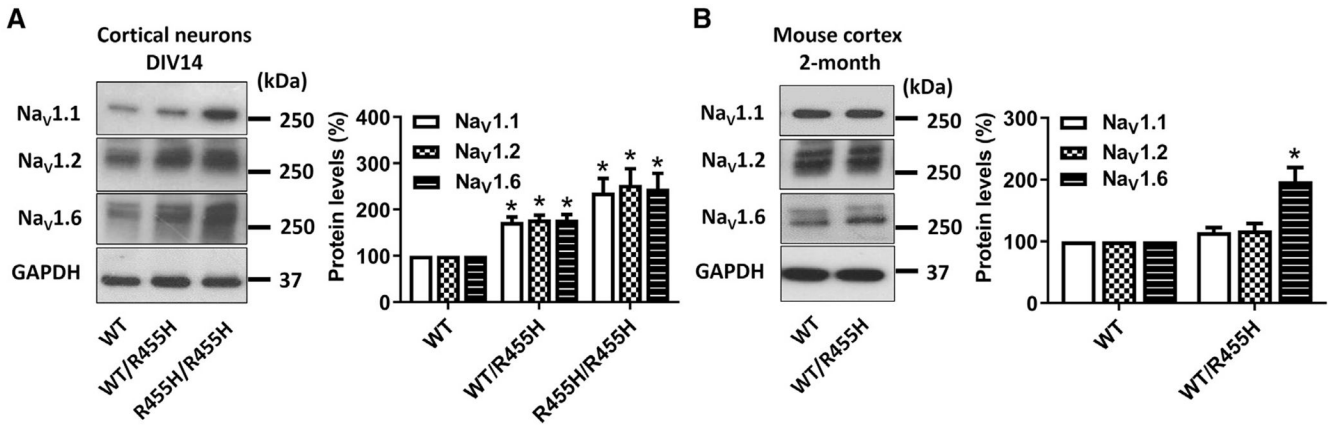

Figure 5. The *Slack-R455H* mutation upregulates Na$_V$ channel subunit expression

(A) Representative western blotting and quantitative analysis of protein levels of Na$_V$1.1, Na$_V$1.2, and Na$_V$1.6 in cultured cortical neurons on DIV 14 obtained from WT, *Slack*$^{+/R455H}$, and *Slack*$^{R455H/R455H}$ littermates. Data are shown as mean ± SEM (n = 4 cultures, 1-way ANOVA).

(B) Representative western blotting and quantitative analysis of protein levels of Na$_V$1.1, Na$_V$1.2, and Na$_V$1.6 in cerebral cortex of 2-month-old WT and *Slack*$^{+/R455H}$ mice. Data are shown as mean ± SEM (n = 4 mice, Student's t test). *p < 0.05.

Author Manuscript Author Manuscript Author Manuscript Author Manuscript

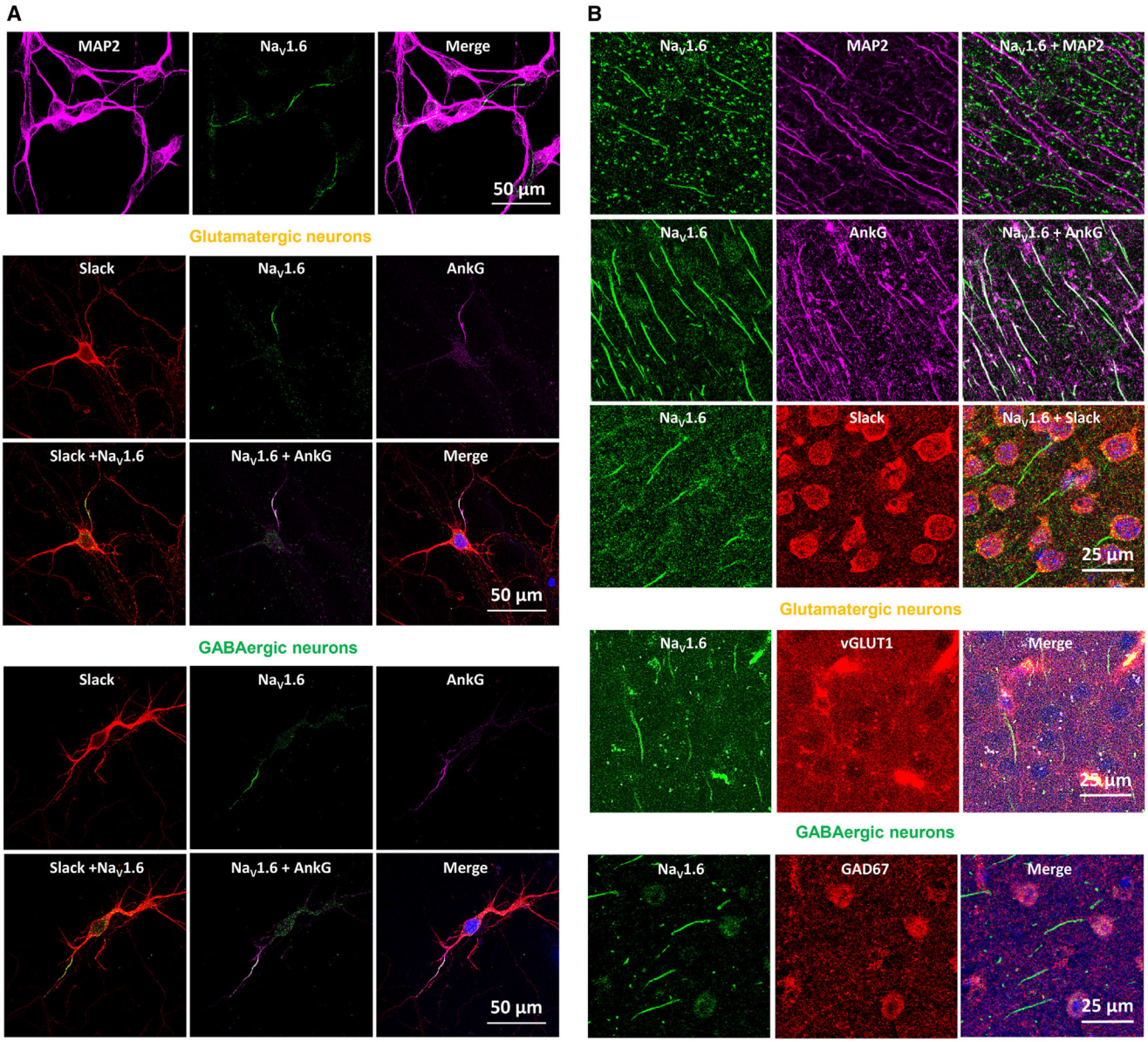

Figure 6. Subcellular localizations of Slack and $Na_V1.6$ channels

(A) Immunostaining of Slack and $Na_V1.6$ with the dendrite (MAP2) and AIS (AnkG) markers in cultured cortical neurons on DIV 14. Glutamatergic and GABAergic neurons were differentiated according to their morphological features. Scale bar, 50 μm.

(B) Immunostaining of Slack and $Na_V1.6$ with MAP2 and AnkG in cerebral cortex of 2-month-old mice (top). Glutamatergic (center) and GABAergic (bottom) neurons were differentiated by coimmunostaining with VGlut1 and GAD67. Scale bar, 25 μm.

See also Figures S3 and S4.

Author Manuscript Author Manuscript Author Manuscript Author Manuscript

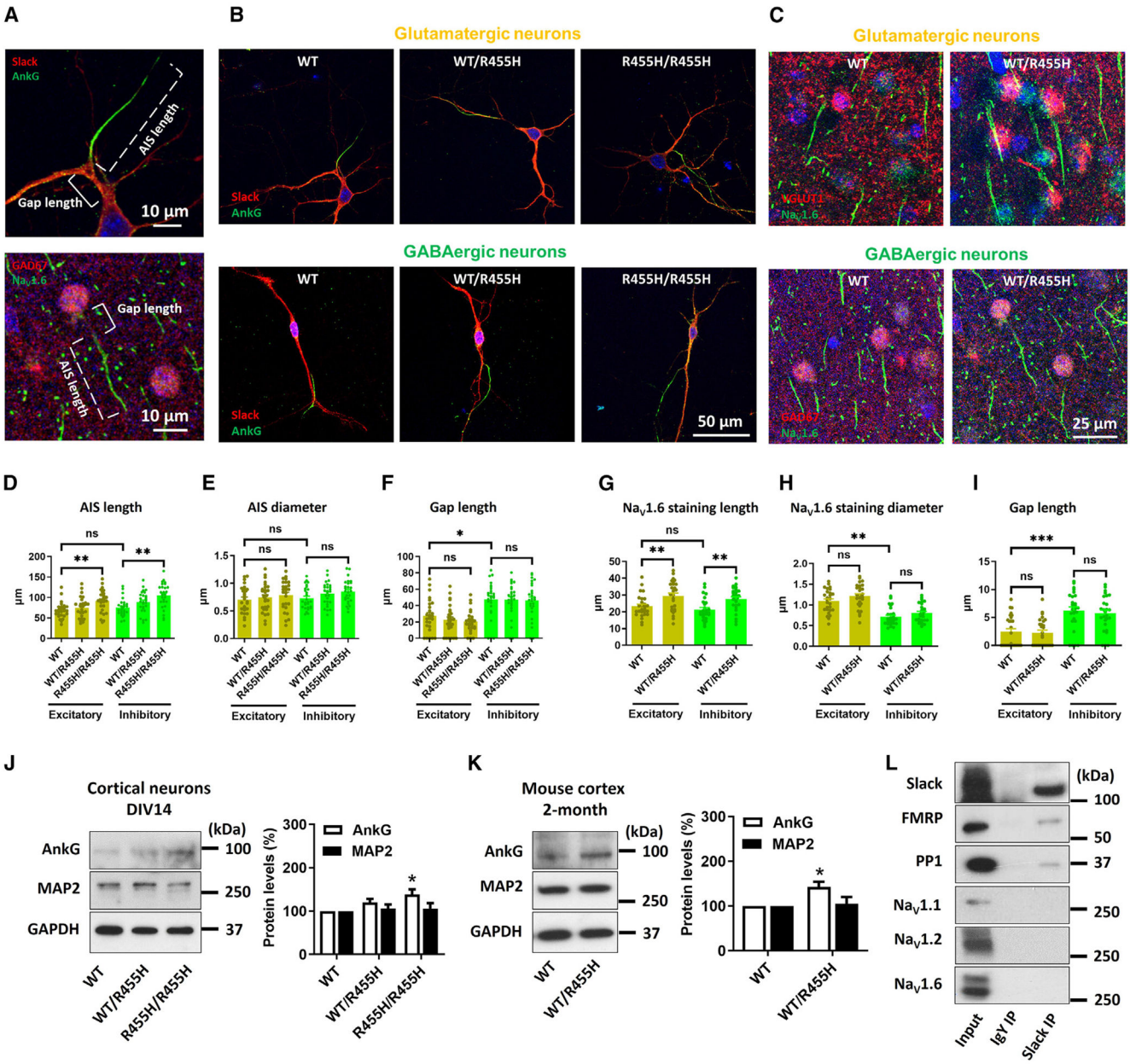

Figure 7. The *Slack-R455H* mutation alters the AIS length of both glutamatergic and GABAergic neurons

(A) Representative high-magnification images of a single neuron for quantification of the AIS length, AIS diameter, and gap length. Dashed line: AIS length; solid line: gap length. Scale bar, 10 μm.

(B) Representative images of single neurons and their AISs (green, AnkG) for cortical glutamatergic neurons (top) and GABAergic neurons (bottom) on DIV 14. Scale bar, 50 μm.

(C) Representative images of neurons and their AISs (green, $Na_V1.6$ staining) for pyramidal cells (red, VGlut1) and interneurons (red, GAD67) from layer II/III of the frontal cortex of 2-month-old mice. Scale bar, 25 μm.

Author Manuscript Author Manuscript Author Manuscript Author Manuscript

(D–F) Quantification of overall AIS length (D), AIS diameter (E), and gap length (F) in excitatory glutamatergic neurons (yellow) and inhibitory GABAergic neurons (green). Data are shown as mean ± SEM (n = 27 AISs, 1-way ANOVA for different genotypes within each neuron type and Student's t test for different neuron types within each genotype). Each symbol represents an individual AIS.

(G–I) Quantification of overall AIS length (G), AIS diameter (H), and gap length (I) in excitatory pyramidal (yellow) and interneuron (green) populations. Data are shown as mean ± SEM (n = 27 AISs, Student's t test). Each symbol represents an individual AIS.

(J and K) Representative western blotting and quantitative analysis of protein levels of AnkG and MAP2 in cultured cortical neurons on DIV 14 (J, n = 4 cultures, 1-way ANOVA) and in cerebral cortex of 2-month-old mice (K, n = 4 mice, Student's t test).

(L) Coimmunoprecipitation of Slack and Na_V channels from mouse cerebral cortex. Brain lysates were subjected to immunoprecipitation using anti-Slack antibody or chicken immunoglobulin Y, followed by western blotting with Slack, FMRP, PP1, $Na_V1.1$, $Na_V1.2$, and $Na_V1.6$ antibodies. ns, not significant; *p < 0.05; **p < 0.01; ***p < 0.001.

See also Figure S4.

Author Manuscript Author Manuscript Author Manuscript Author Manuscript

KEY RESOURCES TABLE

REAGENT or RESOURCE	SOURCE	IDENTIFIER
Antibodies		
Mouse anti-KCNT1 (Slack, N3/26)	Neuromab	Cat# 75-051; RRID:AB_2131855
Rabbit anti-KCNT1 (Slack)	Alomone Labs	Cat# APC-124; RRID:AB_10557314
Chicken anti-KCNT1	AvesLabs	N/A
Rabbit anti-SCN1A ($Na_V1.1$)	Alomone Labs	Cat# ASC-001; RRID:AB_2040003
Rabbit anti-SCN2A ($Na_V1.2$)	Alomone Labs	Cat# ASC-002; RRID:AB_2040005
Rabbit anti-SCN8A ($Na_V1.6$)	Alomone Labs	Cat# ASC-009; RRID:AB_2040202
Rabbit anti-GAD67	Abcam	Cat# ab213508; RRID:AB_3076590
Mouse anti-GAD67 (OTI3G9)	Thermo Fisher Scientific	Cat# MA524909; RRID:AB_2723202
Rabbit anti-GluR1	MilliporeSigma	Cat# AB1504; RRID:AB_2113602
Mouse anti-vGLUT1 (CL2754)	Thermo Fisher Scientific	Cat# MA531373; RRID:AB_2787010
Mouse anti-MAP2	Santa Cruz Biotechnology	Cat# SC-32791; RRID:AB_627948
Mouse anti-Ankyrin G (4G3F8)	Thermo Fisher Scientific	Cat# 33-8800; RRID:AB_2533145
Rabbit anti-FMRP	Abcam	Cat# ab17722; RRID:AB_2278530
Mouse anti-PP1(E–9)	Santa Cruz Biotechnology	Cat# SC-7482; RRID:AB_628177
Mouse anti-GAPDH	Santa Cruz Biotechnology	Cat# SC-32233; RRID:AB_627679
Goat anti-Mouse IgG (H + L) Highly Cross-Adsorbed Secondary Antibody, Alexa Fluor 488	Thermo Fisher Scientific	Cat# A11029; RRID:AB_2534088
Goat anti-Rabbit IgG (H + L) Highly Cross-Adsorbed Secondary Antibody, Alexa Fluor 488	Thermo Fisher Scientific	Cat# A-11008; RRID:AB_143165
Goat anti-Chicken IgG (H + L) Highly Cross-Adsorbed Secondary Antibody, Alexa Fluor 488	Thermo Fisher Scientific	Cat# A11039; RRID:AB_2534096
Goat anti-Mouse IgG (H + L) Highly Cross-Adsorbed Secondary Antibody, Alexa Fluor 546	Thermo Fisher Scientific	Cat# A11030; RRID:AB_2534089
Goat anti-Rabbit IgG (H + L) Highly Cross-Adsorbed Secondary Antibody, Alexa Fluor™ Plus 647	Thermo Fisher Scientific	Cat# A32733; RRID:AB_2633282
Chemicals, peptides, and recombinant proteins		
HotStarTaq Plus Master Mix Kit (250)	QIAGEN	Cat# 203643
Pierce BCA Protein Assay Kit	Thermo Fisher Scientific	Cat# 23225
PrecipHen® Immunoprecipitation Reagent	AvesLabs	Cat# P-1010
Tetraethylammonium (TEA)-Cl	Sigma-Aldrich	Cat# 86614
Tetrodotoxin (TTX)	Alomone Labs	Cat# 18660-81-6
Critical commercial assays		
TaqI-v2	New England Biolabs	Cat# R0149S
Poly-L-Lysine Solution (0.01%)	EMD Millipore	Cat# A-005-C
Fetal bovine serum	GE Healthcare	Cat# SH3008803
Neurobasal™ Medium	GIBCO	Cat# 21103049
Penicillin/Streptomycin	GIBCO	Cat# 15140-122
0.5% Trypsin-EDTA	GIBCO	Cat# 25300-054

Author Manuscript Author Manuscript Author Manuscript Author Manuscript

REAGENT or RESOURCE	SOURCE	IDENTIFIER
GlutaMAX	GIBCO	Cat# 35050-061
B27 supplement	GIBCO	Cat# 17504-044
Experimental models: Cell lines		
Primary cortical neurons	This paper	N/A
Experimental models: Organisms/strains		
Mouse: *Slack*$^{+/R455H}$	This paper	N/A
Mouse: C57BL/6J	The Jackson Laboratory	Cat# JAX:000664; RRID:IMSR_JAX:000664
Mouse: GAD67-GFP (G42 line)	The Jackson Laboratory	Strain # 007677; RRID:IMSR_JAX:007677
Oligonucleotides		
Primer: Slack Forward: 5′-ACAGCTGCGGTGAGTTCAGG-3′	This paper	N/A
Primer: Slack Reverse: 5′-GGGAAGGTTGTCCCAAAGGAGAGC-3′	This paper	N/A
Software and algorithms		
pCLAMP Clampex Software	Molecular Devices	https://www.moleculardevices.com/products/axon-patch-clamp-system
LAS X Life Science Microscope Software	Leica Microsystems	https://www.leica-microsystems.com/products/microscope-software/p/leica-las-x-ls/
ImageJ (Fiji)	Eliceiri/LOCI group	https://fiji.sc/
GraphPad Prism version 8.0.0 for Windows	GraphPad Software	https://www.graphpad.com/
Other		
Axon MultiClamp 700B Microelectrode Amplifier	Molecular Devices	N/A
Axon Digidata 1550B Plus HumSilencer	Molecular Devices	Digidata 1550B4